A MICROWAVE INTERFEROMETER FOR MEASURING DIELECTRIC PROPERTIES OF LOW-LOSS SOLIDS

BY

KWOK-TUNG CHIU

A Thesis Submitted in Partial Fulfilment of the Requirements of the

DEGREE OF MASTER OF SCIENCE

in the

DEPARTMENT OF PHYSICS

LAKEHEAD UNIVERSITY

THUNDER BAY, ONTARIO, CANADA

Examiners:

Internal: External:

LAKEHEAD UNIVERSITY

AUGUST, 1974

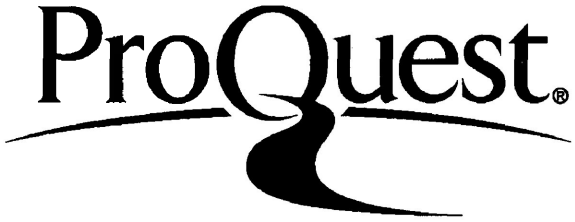

ProQuest LLC.
789 East Eisenhower Parkway
P.O. Box 1346
Ann Arbor, MI 48106 - 1346

Canadian Thesis on Microfiche
No. 24465

ACKNOWLEDGEMENT

I wish to express my gratitude to Dr. D. G. Frood of the Department of Physics for his continued supervision, guidance and support. I am also indebted to Mr. W. Morgan and others in the Department of Chemistry for their valuable assistance.

TABLE OF CONTENTS

		Page
ABSTRACT		1
1.	Introduction	2
Part I.	The Microwave Interferometer	
2.	Apparatus	7
	(a) The Interferometer	8
	(b) The Sample Holder and Heat Bath	10
3.	Theory of the Interferometer for Plane Dielectric Samples	13
4.	Preliminary Measurements and Results on Samples with Known Dielectric Properties	23
5.	Corrections for Low-Loss Materials	28
	(a) Theoretical Improvements	28
	(b) Experimental Improvements	33
6.	Additional Measurements and Results	35
7.	Conclusions and Discussion	36
Part II.	Application of the System: Dielectric Properties of Polystyrene and Dilute solutions of Polar Impurities in Polystyrene	
8.	Introduction	40
	(a) Structure of Polystyrene	40
	(b) Polar Impurities in Polystyrene	41
9.	Preparation of Polystyrene Samples	46
10.	Temperature Dependance of Sample Holder	49

Page

11. Results of Dielectric Measurements 51

(a) Polystyrene 51

(b) Polystyrene weakly doped with 8-Hydroxyquinoline 55

12. Summary and Conclusions 59

APPENDICES A - J: Tables of Data 62

REFERENCES 72

ABSTRACT

An X-band microwave bridge-interferometer is constructed for measuring the permittivity of solids. Using simple theory, the system is first tested with several materials of known permittivity (e.g. ertalon, plexiglas and teflon). It is found that the results agreed well with published data for lossy materials only. Loss factors of very low-loss materials are irregular rather than linear with the sample lengths as is expected. This is due to the fact that the usual simple theory neglects internal multiple reflections which are predominant inside low-loss materials. The problem does not exist in lossy materials because the transmitted signal is sufficiently dissipated through one traverse of the sample. Theoretical correction for low-loss materials is made but is found too tedious to be used. On the other hand, multiple-reflection effects could be eliminated if the samples are cut exactly to multiples of half-wavelengths. Samples of arbitrary lengths have to be used first to obtain a preliminary measurement of the real part of the permittivity which is related to the wavelength of the sample by a simple equation. Fine adjustment of the klystron frequency is also made to ensure minimum reflections by the samples.

The precision method is then employed to study the dielectric properties of pure polystyrene and polystyrene doped with diluted amounts (0.1~2.0%) of polar molecules (viz. 8-Quinolinol) at various temperatures (20°-80°C). It is anticipated that the new data obtained here will provide useful information for the study of dielectric relaxation mechanisms in these substances.

1. Introduction

For weak fields in most materials, the electromagnetic field equations are linear, and the properties of the substance relevant to the study of these equations are completely specified by ε and μ for the given material as shown by Montgomery (1966). These constants are usually separated into real and imaginary parts:

$$\varepsilon = \varepsilon' + i\varepsilon'' = \varepsilon'(1 + i\tan\delta) = \varepsilon_o\varepsilon_r'(1 + i\tan\delta)$$

$$\mu = \mu' + i\mu'' = \mu_o\mu_r'$$

where $\mu_r' \doteq 1$ in most non-magnetic materials. The quantity $\tan\delta$ is called the loss tangent. It equals the ratio of the power dissipated to the power stored per cycle and is thus a measure of the energy lost in the form of heat when an electromagnetic wave is propagated through the material. The dimensionless quantity ε_r', is simply the dielectric constant relative to free space. Since:

$$\varepsilon_o = 8.854185 \times 10^{-12} \text{ F/m} = \text{dielectric constant of free space}$$

and

$$\mu_o = 4\pi \times 10^{-7} \text{ henry/m} = \text{permeability of free space}$$

it is clear that the quantities ε_r' and $\tan\delta$ may be used to specify the properties of most linear, non-magnetic materials.

The micorwave interferometer has long been used to measure dielectric properties of materials, especially in the liquid state as given by Harvey (1963). However, techniques

involved in using this method vary according to the specimens to be measured. Generally the interferometer method is satisfactory due to its simplicity both in theory and experiment. It is especially suitable for measuring medium- to high-loss dielectric materials because the signal transmitted by the first surface of the dielectric is sufficiently dissipated in one traverse of the sample rather than being multiply reflected. In very low-loss dielectrics the opposite situation occurs, much of the signal is unattenuated, resulting in multiple reflections in the dielectric. By using simple theory the resultant dissipation factor, tan δ is thus higher than expected, and it is necessary to provide either an elaborate theoretical correction to the simple formula usually employed in interpreting measurements made with the interferometer or seek an extension of the experimental method to achieve accurate results for the dissipation in low-loss media.

In Part I of this thesis an X - band interferometer is constructed for measuring the permittivity of solids. The usual theory neglects internal, multiple reflections and for plane samples leads to a transmission coefficient:

$$T = e^{i(k' - k_g)d} \cdot e^{-k''d} \qquad \text{(i)}$$

where $k = k' + ik''$ is the propagation constant in the dielectric filled guide, k_g that in the empty guide and d the length of the sample. Since k is related to the permittivity, $\varepsilon_r = \varepsilon_r' + i\varepsilon_r''$ through:

$$k^2 = \left(\frac{2\pi}{\lambda_o}\right)^2 \left[\varepsilon_r - \left(\frac{\lambda_o}{\lambda_c}\right)^2 \right] \qquad \text{(ii)}$$

where λ_o and λ_c are the free space and cut-off wavelengths, respectively, ε_r' and ε_r'' are given in terms of the measured phase shift, θ (radians) and attentuation, α (db) by:

$$\varepsilon_r' = \left[\sqrt{1 - \left(\frac{\lambda_o}{\lambda_c}\right)^2} + \frac{\lambda_o}{d}\left(\frac{\theta}{2\pi} \pm n\right) \right]^2 - \left(\frac{\alpha\lambda_o}{17{\cdot}372\pi d}\right)^2 + \left(\frac{\lambda_o}{\lambda_c}\right)^2 \qquad \text{(iii)}$$

$$\varepsilon_r'' = \frac{\alpha\lambda_o}{8{\cdot}686\pi d} \left[\sqrt{1 - \left(\frac{\lambda_o}{\lambda_c}\right)^2} + \frac{\lambda_o}{d}\left(\frac{\theta}{2\pi} \pm n\right) \right] \qquad \text{(iv)}$$

where n = integer. Using materials of known permittivity, the measured values agreed well with published data only for lossy dielectrics (eg., ertalon), but for very low-loss materials (eg., teflon, plexiglas) measured losses were two or three orders of magnitude higher than the accepted values. There were two reasons for this discrepancy:

(a) Formula (i) neglects multiple reflections. This approximation is acceptable for lossy materials, but for low-loss dielectrics multiple reflections must be taken into account leading to the exact formula (see § 3):

$$T = (1 - R_\infty^2)\, \frac{e^{i(k - k_g)d}}{1 - R_\infty^2 e^{2ikd}} \qquad \text{(v)}$$

where R_∞ is the reflection coefficient at normal incidence of an unbounded semi-infinite slab of the dielectric.

(b) The theory also assumes there is a single incident and reflected wave from the first face of the sample, and a single transmitted wave from the second. Although every effort was made to establish these conditions (see § 2), reflections (V·S·W·R· $\simeq$ 1·1) from both the generator-end and the detector end of the sample arm were always present.

To overcome both difficulties (a) and (b), the reflection coefficient of the sample was reduced to as low a value as possible by first making a preliminary measurement of ϵ_r' using arbitrary sample lengths and employing (i) and (iii). Next the samples were cut to an integral number of half-wavelengths (in the dielectric filled guide). With $d = m\lambda/2$ (m = integer), (v) reduces to (i), and (iii) and (iv) apply exactly. Employing fine tuning of the klystron, new measurement on half-wavelength samples lead to ϵ_r' and ϵ_r'' for teflon and plexiglas in good agreement with published data. As applied to ertalon, half-wavelength measurements lead to no significant improvements over those for samples of arbitrary length.

Part II of this thesis employs the precision method developed in Part I to study solid, low-loss materials of unknown permittivity. Here we are interested in polystyrene containing dilute amounts (0.1 ~ 2.0 %) of polar molecules; viz, 8 - Quinolinol. The technique for fabricating samples is discussed in § 9 and the results of measurement of ϵ_r' and ϵ_r'' at various temperatures (20° - 80°) are given in § 11.

It is anticipated that the new information obtained here at X - band frequencies will eventually be correlated with measurements from other microwave bands and with existing r.f. and low-frequency data to obtain complete, temperature - dependent dispersion curves for these substances.

PART 1

The Microwave Interferometer for Measuring Dielectric Properties of Solids

2. Apparatus

(a) The Interferometer

The microwave system used here is called a bridge-interferometer in that the output from a signal generator is divided equally into the two arms of a waveguide bridge. One arm contains the sample under test, the other (the reference arm) a precision phase shifter and an attenuator. These instruments are adjusted to give balance and the difference in readings due to the presence of the sample are measured directly. Hence $\varepsilon_r = \varepsilon_r' + i\varepsilon_r''$ may be calculated.

A block diagram of the interferometer is shown in Figure 1. Electromagnetic radiation is generated by a klystron which is energized by the Klystron Power Supply. This power source provides a regulated, d-c, adjustable voltage for operation of the beam electrode of the klystron. It also provides voltage for the operation of the reflector electrode. A fan is necessary here to cool and stablize the temperature of the klystron. The reflector output is modulated by an internally-generated 1000-cycle square wave. The signal propagates along a rectangular waveguide in the $TE_{0,1}$ mode. An isolator is placed next to the klystron to prevent reflections from reaching the klystron and thereby affecting the output frequency. The variable attenuator which follows adjusts the level of energy flowing to the rest of the system. The directional coupler is connected to the frequency meter as shown. The latter, in

Figure 1.

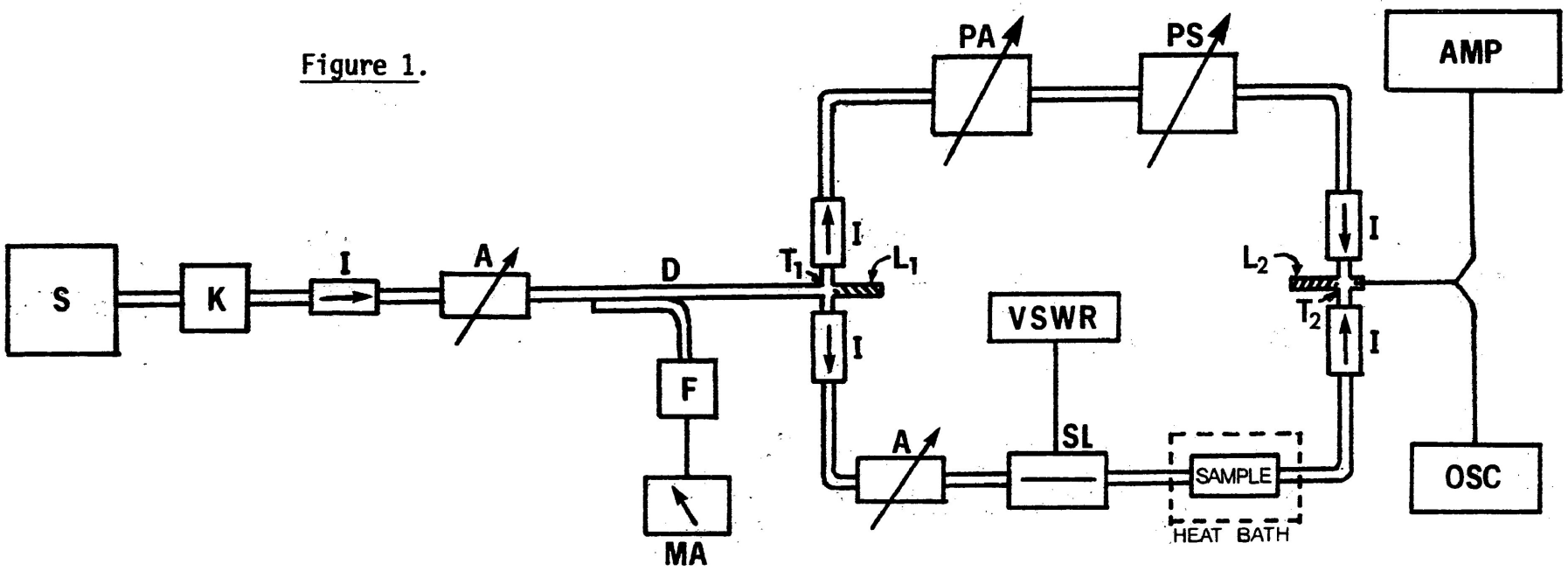

A	Level Setting Attenuator, H. P. Model X375A
AMP	Lock-in Amplifier, H.P. Model 128
D	Directional Coupler, 20 db, H.P. Model X752D
F	Waver Meter, H. P. Model X532B
I	Isolator, FXR Model X157A
K	Klystron, Western Electric Model 2K25 723A/B, 25mw.
L_1,L_2	Match Loads, H. P. Model X910B
MA	Microammeter
OSC	Oscilloscope, H. P. Model 130C
PA	Precision Attenuator, H. P. Model X382A
PS	Phase Shifter, H. P. ModelX885A
S	Klystron Power Supply, H.P. Model 716B
SL	Slotted Line with Carriage,H.P.Model 809C
T_1,T_2	Magic Tees
VSWR	Standing Wave Indicator, H.P.Model 415BR

connection with a crystal detector and a microammeter, measures the frequency of the wave signal. This is done by tuning the wavemeter until the microammeter shows a sudden drop of current--indicating the cavity to be in resonance. Next a magic-tee splits the output of the main signal into two arms. One arm passes through a variable attenuator followed by the Standing Wave Ratio Indicator and then the sample; the reference arm incorporates a calibrated rotatory vane attenuator and a precision phase shifter. Isolators are placed at the two ends of both arms to prevent reflections. The signals from the two arms are recombined by another magic-tee and pass to a crystal detector and an oscilloscope on which a square wave could be observed. By adjusting the precision phase shifter and attenuator the square wave could be reduced to a straight line indicating the bridge to be balanced. A matched load is attached to the third arm of each magic-tee to absorb the power passing into that arm.

Because of the low power of the source (25 m.w.), the oscilloscope had insufficient sensitivity, and a lock-in amplifier was used here as a null detector in parallel with the oscilloscope. The main feature of this instrument is that it can measure very weak signals (sensitivity 1 μV) which are "buried in noise". The reference signal required by the amplifier is obtained from the synchronized output of the Klystron Power Supply.

Finally, the sample holder is temperature controlled by a heat bath which encloses it.

(b) The Sample Holder and Heat Bath

The sample holder was constructed as follows: Two pieces of brass were soldered to the side walls of the waveguide as shown in Figure 2. The top of the soldered piece was then milled off (Figure 2b) and replaced by a rectangular piece of brass. Holes were then drilled through the cover to each of the soldered and tapped brass side bars. The alignment of the holes is such that the screws could be inserted only if the hole positions between the cover and the guide are matched (Figure 2e). In order that the pressure between the two pieces be consistent every time the holder is reassembled, the cover and the washers were marked--the washers being soldered to the bolt heads.

The heat bath is constructed of a 4"-diameter brass cylinder wrapped with layers of asbestos. Between the layers, a length of nichrome wire was coiled and the two ends of the wire were connected to a variable transformer (variac). The ends of the cylinder were closed by asbestos windows through which a thermometer could be inserted (Figure 3).

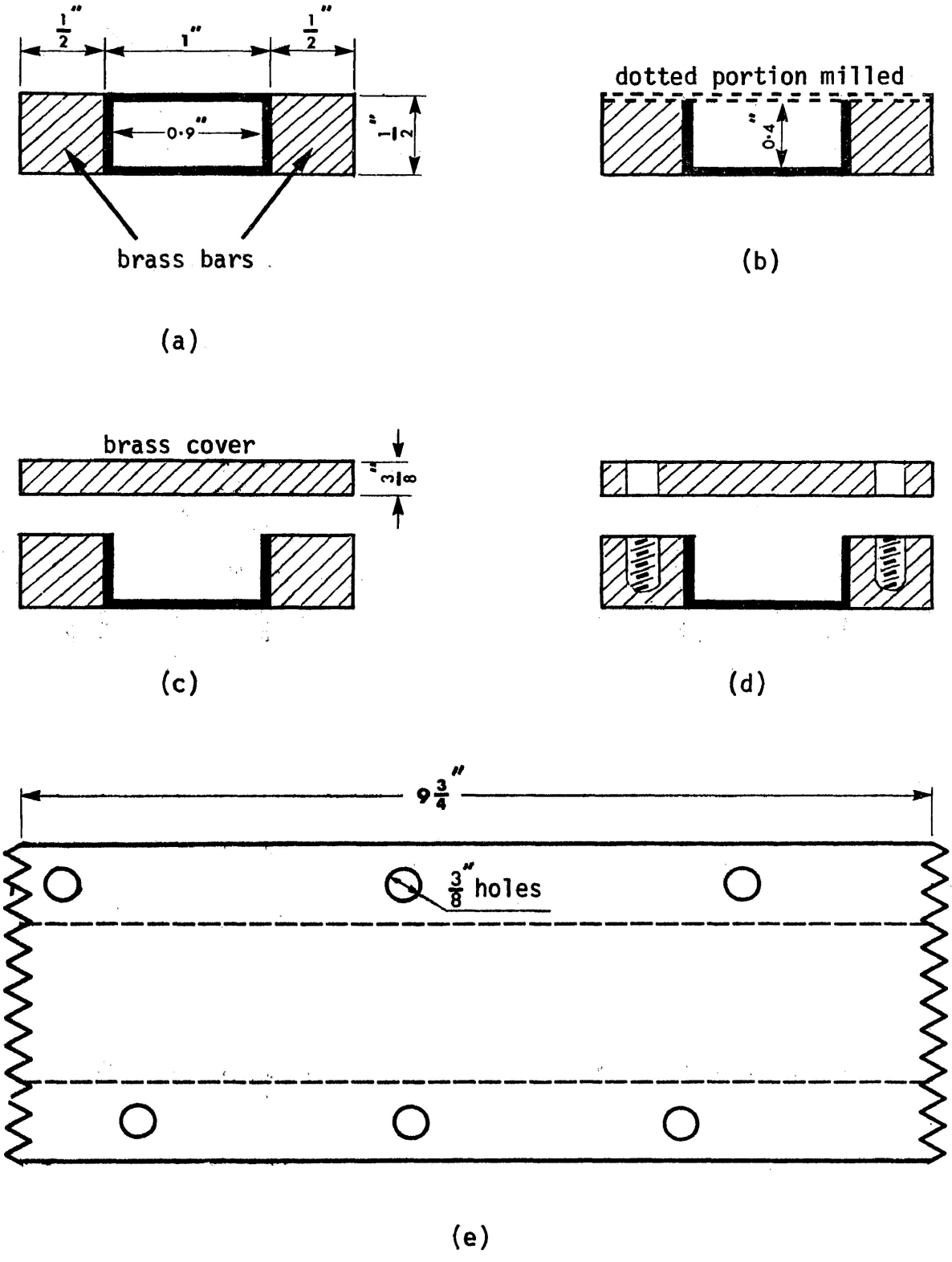

Figure 2. Procedures of making the sample holder.

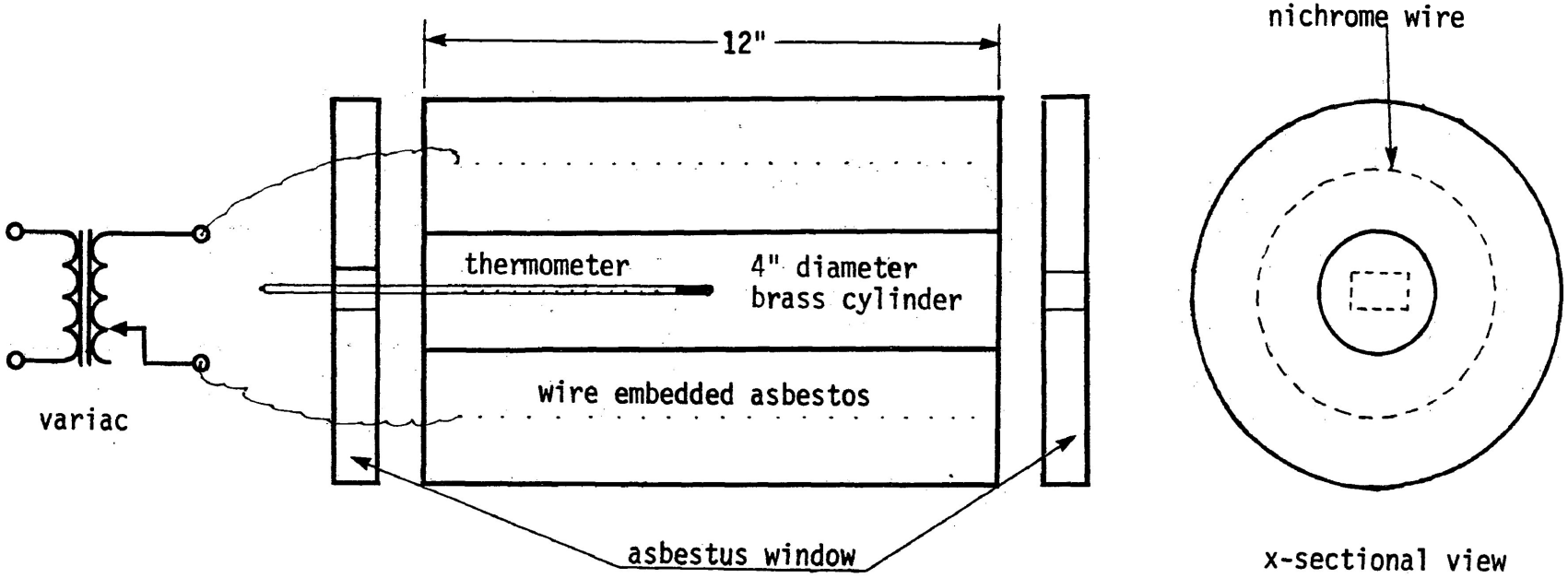

Figure 3. Heat Bath.

3. Theory of the Interferometer for Plane Samples

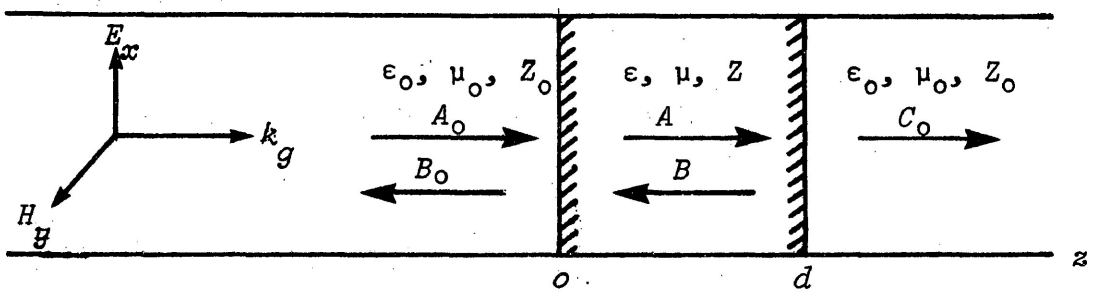

Figure 4.

Assuming that the guide is operated in the $TE_{0,1}$ mode, the electric field has a sinusoidal distribution in the y - direction, thus according to Fuller (1947),

$$E_x = E_o e^{i(\omega t + k_g z)} \sin \frac{\pi y}{a}$$

where a is the width of the guide and k_g is the propagation constant in the waveguide in vacuum.

Referring to Figure 4, the electric and magnetic fields of the wave incident on a plane sample of dielectric of length d are:

$$E_i = A_o e^{i(\omega t + k_g z)} \sin \frac{\pi y}{a}$$

$$H_i = \frac{A_o}{Z_o} e^{i(\omega t + k_g z)} \sin \frac{\pi y}{a} .$$

For the reflected wave, the fields at $z = o$ are:

$$E_r(o) = B_o e^{i(\omega t - k_g z)} \sin \frac{\pi y}{a}$$

$$H_r(o) = \frac{-B_o}{Z_o} e^{i(\omega t - k_g z)} \sin \frac{\pi y}{a}$$

and from the second face ($z = d$) the fields of the transmitted wave are:

$$E_t(d) = C_o\, e(\omega t + k_g z)\, \sin \frac{\pi y}{a}$$

$$H_t(d) = \frac{C_o}{Z_o}\, e^{i(\omega t + k_g z)}\, \sin \frac{\pi y}{a} \quad .$$

Inside the dielectric slab, the transmitted wave from the first plane and the reflected wave from the second plane are respectively:

$$\begin{cases} E_t(o) = Ae^{\,i(\omega t + kz)}\, \sin \frac{\pi y}{a} \\ H_t(o) = \frac{A}{Z}\, e^{\,i(\omega t + kz)}\, \sin \frac{\pi y}{a} \end{cases},$$

$$\begin{cases} E_r(d) = Be^{\,i(\omega t - kz)}\, \sin \frac{\pi y}{a} \\ H_r(d) = \frac{-B}{Z}\, e^{\,i(\omega t - kz)}\, \sin \frac{\pi y}{a} \end{cases}.$$

The constants A_o, B_o, A, B, and C_o in the above equations are the amplitudes of the waves; Z_o and Z are the characteristic impedences of the empty guide and the dielectric filled guide respectively, and k_g and k are the propagation constants of the corresponding waves.

The total fields in the different regions are therefore as follows:

For $z < 0$

$$E_x = \left[A_0 e^{ikgz} + B_0 e^{-ikgz} \right] e^{i\omega t} \sin\left(\frac{\pi y}{a}\right)$$

$$H_y = \frac{1}{Z_0} \left[A_0 e^{ikgz} - B_0 e^{-ikgz} \right] e^{i\omega t} \sin\left(\frac{\pi y}{a}\right)$$

For $0 \leq z \leq d$

$$E_x = \left[Ae^{ikz} + Be^{-ikz} \right] e^{i\omega t} \sin\left(\frac{\pi y}{a}\right)$$

$$H_y = \frac{1}{Z} \left[Ae^{ikz} - Be^{-ikz} \right] e^{i\omega t} \sin\left(\frac{\pi y}{a}\right)$$

and for $z > d$

$$E_x = \left[C_0 e^{ikgz} \right] e^{i\omega t} \sin\left(\frac{\pi y}{a}\right)$$

$$H_y = \frac{1}{Z_0} \left[C_0 e^{ikgz} \right] e^{i\omega t} \sin\left(\frac{\pi y}{a}\right) .$$

The reflection coefficient, R and transmission coefficient, T, of the dielectric slab are defined as follows:

$$R = \frac{B_0}{A_0} \quad , \quad T = \frac{C_0}{A_0}$$

The electromagnetic fields satisfy certain boundary conditions as shown by Bronwell (1947). One of these requires that the tangential components of electric intensity are continuous across the boundary. Another states that the tangential component of the magnetic intensity is equal to the surface current density. In all cases, except that of a perfect conductor, the surface density is zero, and the tangential magnetic intensities are continuous. Applying these conditions at the boundaries, we

have for $z = 0$,

$$A_o + B_o = A + B \tag{1}$$

$$A_o - B_o = \frac{Z_o}{Z}(A - B) \tag{2}$$

and for $z = d$,

$$Ae^{ikd} + Be^{-ikd} = C_o e^{ik_g d} \tag{3}$$

$$Ae^{ikd} - Be^{-ikd} = \frac{Z}{Z_o} C_o e^{ik_g d} \tag{4}$$

Eliminating C_o from (3) and (4) gives

$$Ae^{ikd} + Be^{-ikd} = \frac{Z_o}{Z}(Ae^{ikd} - Be^{-ikd})$$

and by rearranging terms,

$$(1 - \frac{Z_o}{Z}) Ae^{ikd} + (1 + \frac{Z_o}{Z}) Be^{-ikd} = 0$$

so that

$$\frac{A}{B} = - (\frac{Z + Z_o}{Z - Z_o}) e^{-2ikd} \tag{5}$$

The quantity

$$R_\infty = \frac{Z - Z_o}{Z + Z_o} \tag{6}$$

is the reflection coefficient of a semi-infinite dielectric slab inside the waveguide as defined by Wheeler (1963). Therefore (5) becomes using (6)

$$\frac{B}{A} = - R_\infty e^{2ikd} \quad . \tag{7}$$

Adding and substracting (1) and (2) gives

$$2B_o = A(1 - \frac{Z_o}{Z}) + B(1 + \frac{Z_o}{Z})$$

$$2A_o = A(1 + \frac{Z_o}{Z}) + B(1 - \frac{Z_o}{Z})$$

Therefore,

$$\frac{B_o}{A_o} = \frac{A(Z - Z_o) + B(Z + Z_o)}{A(Z + Z_o) + B(Z - Z_o)}$$

$$= \frac{R_\infty + \frac{B}{A}}{1 + \frac{B}{A} R_\infty} \quad . \tag{8}$$

Substituting (7) into (8) gives the reflection coefficient of the sample:

$$R = \frac{B_o}{A_o} = R_\infty \left(\frac{1 - e^{2ikd}}{1 - R_\infty^2 e^{2ikd}}\right) \tag{9}$$

Note in (9) that as $d \to \infty$, $R \to R_\infty$.

To obtain the transmission coefficient, add and subtract (3) and (4) to give:

$$A = \frac{C_o}{2} (1 + \frac{Z}{Z_o}) e^{i(k_g - k)d}$$

$$B = \frac{C_o}{2} (1 - \frac{Z}{Z_o}) e^{i(k_g + k)d}$$

and since from (1),

$$A + B = A_o + B_o$$

$$= A_o(1 + R)$$

it follows that :

$$A_o(1 + R) = \frac{C_o}{2}\left[(1 + \frac{Z}{Z_o}) + (1 - \frac{Z}{Z_o})e^{2ikd}\right]e^{i(k_g - k)d}$$

that is

$$\frac{C_o}{A_o} = \frac{2(1 + R)e^{i(k - k_g)d}}{(1 - R_\infty e^{2ikd})(1 + \frac{Z}{Z_o})} \qquad (10)$$

But from (9), the definition of R, it is seen that:

$$\frac{1 + R}{1 - R_\infty e^{2ikd}} = \frac{1 + \dfrac{R_\infty - R_\infty e^{2ikd}}{1 - R_\infty^2 e^{2ikd}}}{1 - R_\infty e^{2ikd}}$$

$$= \frac{(1 + R_\infty) - R_\infty(1 + R_\infty)e^{2ikd}}{(1 - R_\infty e^{2ikd})(1 - R_\infty^2 e^{2ikd})}$$

$$= \frac{1 + R_\infty}{1 - R_\infty^2 e^{2ikd}} \quad .$$

Therefore (10) becomes

$$\frac{C_o}{A_o} = \frac{2(1 + R_\infty)e^{i(k - k_g)d}}{(1 + \frac{Z}{Z_o})(1 - R_\infty^2 e^{2ikd})} \tag{11}$$

but:

$$\frac{2(1 + R_\infty)}{1 + \frac{Z}{Z_o}} = 1 - (\frac{Z - Z_o}{Z + Z_o})^2 = 1 - R_\infty^2$$

so (11) becomes,

$$\boxed{T = \frac{C_o}{A_o} = \frac{1 - R_\infty^2}{1 - R_\infty^2 e^{2ikd}} e^{i(k - k_g)d}} \quad . \tag{12}$$

For $R_\infty^2 << 1$, (as usually the case for most dielectrics), (12) becomes:

$$T \doteq e^{i(k - k_g)d}$$

$$\boxed{T \doteq e^{i(k' - k_g)d} \; e^{-k''d}} \tag{13}$$

where k, a complex quantity, is defined as $k = k' + ik''$. Since (13) is a good approximation for the case of small reflection coefficient R_∞, it will be used here initially instead of (12). The result (13) is the usual formula employed in interpreting interferometer measurements. It

can be understood by saying that the wave is shifted through a phase $(k' - k_g) \pm 2n\pi$ where n is any integer, and attenuated by an amount $e^{-k''d}$. Essentially, (13) is the result that would be obtained had multiple reflections inside the dielectric been ignored. The phase shift is expressed in radians and the attenuation in nepers. The more common unit of attenuation, however, is the decibel. 1 neper = 8.686 decibels. Hence,

$$\theta = (k' - k_g)d \pm 2n\pi \quad \text{(radian)}$$

$$\alpha = -20 \log_{10}|T| \quad (db)$$

$$= 8.686\, k''d \quad (db) \quad . \tag{14}$$

We are now in a position to relate θ and α to the dielectric constant $\varepsilon_r = \varepsilon_r' + i\varepsilon_r''$. Using the wave equation, eg., Barnes (1965):

$$\frac{\partial^2 E_x}{\partial x^2} + \frac{\partial^2 E_x}{\partial y^2} + \frac{\partial^2 E_x}{\partial z^2} = -k_o^2 E_x$$

where k_o, the propagation constant in unbounded dielectric is given by $k_o = \omega\sqrt{\mu\varepsilon}$, we substitute the definition for E_x inside the dielectric slab into the wave equation, resulting in:

$$k^2 = k_o^2 - \left(\frac{\pi}{a}\right)^2$$

$$= \omega^2\mu\varepsilon - \left(\frac{\pi}{a}\right)^2 \quad . \tag{15}$$

Notice that $k = o$ if $\omega^2\mu\epsilon = (\frac{\pi}{a})^2$ or:

$$\omega\sqrt{\mu\epsilon} = \frac{2\pi\nu}{v} = \frac{2\pi}{\lambda} = \frac{\pi}{a}$$

where $v = \frac{1}{\sqrt{\mu\epsilon}}$ is the phase velocity in the dielectric. That is, cutoff occurs at a wavelength $\lambda_c = 2a$. Wavelengths greater than λ_c are evanescent. Since,

$$k_o^2 = \omega^2\mu\epsilon = \omega^2\mu_o\epsilon_o\epsilon_r = (\frac{2\pi}{\lambda_o})^2 \epsilon_r$$

(15) becomes

$$k^2 = (\frac{2\pi}{\lambda_o})^2\left[\epsilon_r - (\frac{\lambda_o}{\lambda_c})^2\right] .$$

Separating this last result into real and imaginary parts,

$$k'^2 - k''^2 + 2ik'k'' = (\frac{2\pi}{\lambda_o})^2(\epsilon_r' + i\epsilon_r'')-(\frac{2\pi}{\lambda_o})^2(\frac{\lambda_o}{\lambda_c})^2$$

we find ϵ_r' and ϵ_r'' explicitly as:

$$\epsilon_r' = (k'^2 - k''^2)(\frac{\lambda_o}{2\pi})^2 + (\frac{\lambda_o}{\lambda_c})^2 \qquad (16)$$

$$\epsilon_r'' = 2k'k''(\frac{\lambda_o}{2\pi})^2. \qquad (17)$$

Solving (14) for k' and k'' we obtain:

$$k' = \frac{\theta \pm 2n\pi}{d} + k_g$$

$$k'' = \frac{\alpha}{8.686d}$$

and substituting these into (16) and (17) give:

$$\varepsilon_r' = \left[\frac{\lambda_o(\theta \pm 2n\pi)}{2\pi d} + \sqrt{\left(1 - \frac{\lambda_o}{\lambda_c}\right)^2} \right]^2 - \left(\frac{\alpha\lambda_o}{2\times 8.686\pi d}\right)^2 + \left(\frac{\lambda_o}{\lambda_c}\right)^2 \tag{18}$$

$$\varepsilon_r'' = \left[\frac{\lambda_o(\theta \pm 2n\pi)}{2\pi d} + \sqrt{\left(1 - \left(\frac{\lambda_o}{\lambda_c}\right)^2\right)} \right] \frac{\alpha\lambda_o}{8.686\pi d} \tag{19}$$

where

$$\lambda_g = \frac{2\pi}{k_g} = \frac{\lambda_o}{\sqrt{1 - \left(\frac{\lambda_o}{\lambda_c}\right)^2}} \tag{20}$$

is the wavelength in the empty waveguide.

As a check of (18) and (19), let $\lambda_g = \lambda_o$ in (20) -- which implies that λ_c goes to infinity as would be the case were the dielectric unbounded. (18) and (19) become:

$$\varepsilon_r' = \left[\frac{\lambda_o}{d}\left(\frac{\theta}{2\pi} \pm n\right) + 1 \right]^2 - \left(\frac{\alpha\lambda_o}{2\times 8.686\pi d}\right)^2 \tag{21}$$

$$\varepsilon_r'' = \left[\frac{\lambda_o}{d}\left(\frac{\theta}{2\pi} \pm n\right) + 1 \right] \frac{\alpha\lambda_o}{8.686\pi d} \tag{22}$$

and (21) and (22) are identical to those for an unbounded dielectric slab derived by Frood (1964).

4. Preliminary Measurements and Results on Samples with Known Dielectric Properties

The behaviour of the apparatus discussed in § 2 was tested by using plane samples of known dielectric properties; viz., teflon, plexiglas and ertalon.

Samples of a given material are cut into different lengths and fitted into the waveguide in different combinations. Different readings of phase shift and attenuation are noted. The "zero point" readings are also noted with the waveguide empty. The difference between the former and the latter gives the phase shift and attenuation of the sample.

The free space wavelength, λ_o, used in (18) and (19) was found by the relation $\lambda_o = c_o/f$ where c_o is the speed of light in vacuum and f the frequency shown by using the slotted line which gives the wavelength of the signal in the waveguide, λ_g. These two wavelengths, λ_o and λ_g fit relation (20).

In the present measurements, the distance between the sample and the source must remain constant as the sample length is increased. A linear plot of attenuation and phase shift against sample length is required for satisfactory and sensible interpretation of the results of the measurements.

Using the approximate formula (13), ertalon was found to have a room temperature dielectric constant of 3.40 ± 0.6% and a loss tangent of 0.0217 ± 2.7% at 8.64 GHz. Although we have

no exact reference as to its dielectric properties, these results are comparable with those found in the Johnston Industrial Plastics (1970). Furthermore, a plot of θ and α *versus* sample length (see Figure 5) are staight lines within experimental errors.

Again using (13) the dielectric constants of teflon and plexiglas were found to be 1.97 ± 1.5% and 2.54 ± 1.8% respectively at 9.547 GHz. These results are extremely close to the published results as shown by Von Hippel (1954). The phase shifts due to the samples are also found to be linear with length as shown in Figure 6. However, the calculated loss tangents for both samples are very much higher than expected. These values are not accurate since, as shown in Table 1, the losses appear to be highly non-linear with the sample length. In fact, the attentuations were found to be fluctuating with minima occurred at approximately regular intervals of length (Figure 7).

The reason for the unsatisfactorily results with respect to loss measurements is believed to be due to the fact that both teflon and plexiglas are very low-loss materials; much of the signal transmitted by the first face of the dielectric was unattenuated rather than being dissipated as heat, resulting in multiple reflections in the dielectric and the inapplicability of equation (13). This being the case, some correction has to be made for low-loss materials--either theoretically or experimentally.

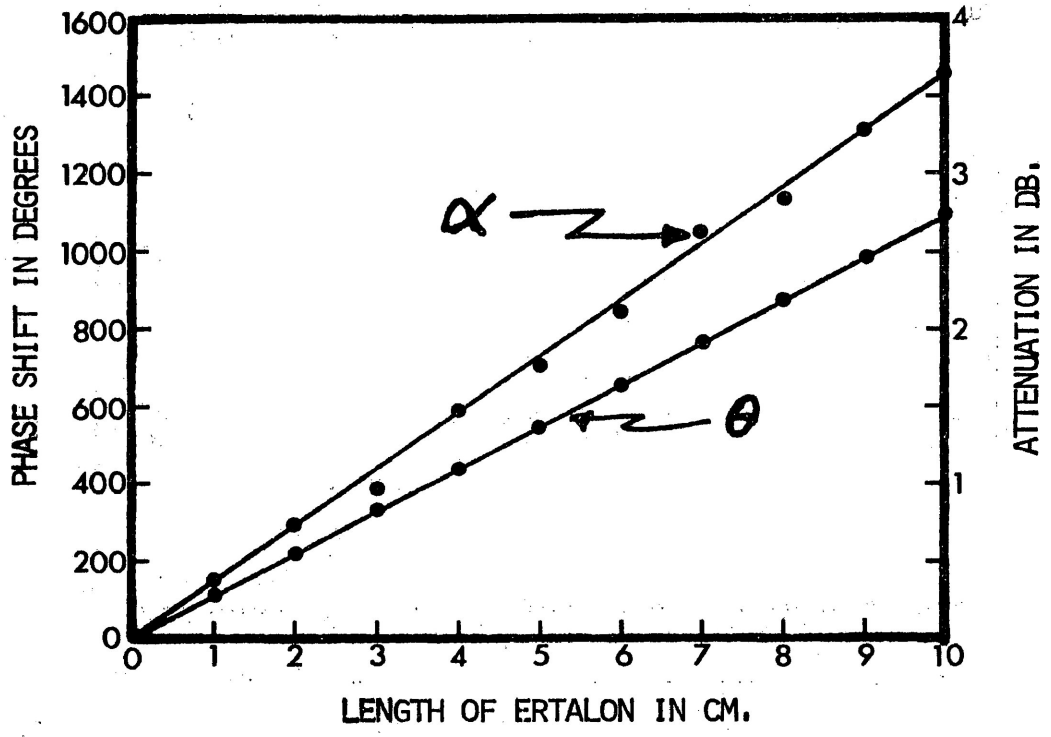

Figure 5. Phase shift and attenuation of ertalon as a function of sample length.

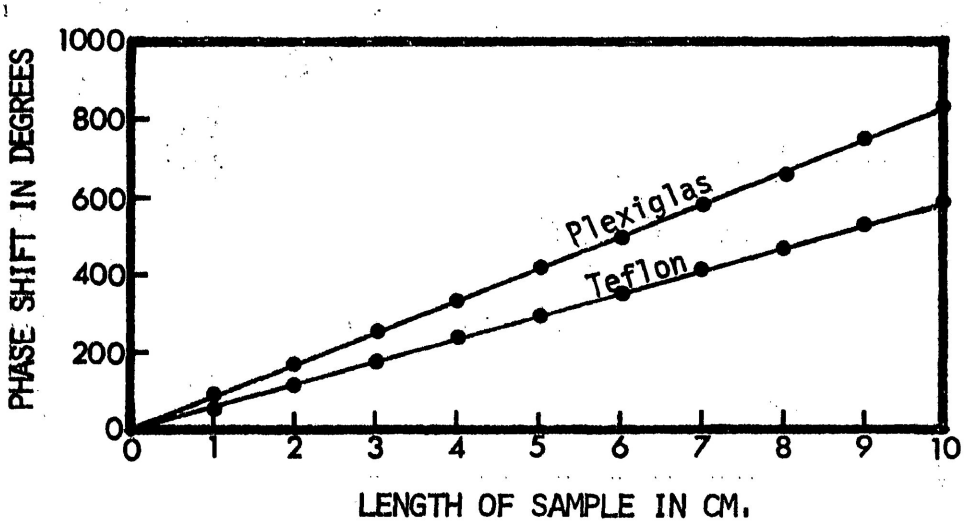

Figure 6. Phase shifts of teflon and plexiglas as a function of sample length.

Preliminary Measurements of Dielectric Properties of:

	Ertalon				Plexiglas				Teflon			
	Frequency = 9.08 GHz				Frequency = 9.547 GHz				Frequency = 9.547 GHz			
d cm	θ *degree*	α *db*	ε'_r	tan δ x 10^{-4}	θ *degree*	α *db*	ε'_r	tan δ x 10^{-4}	θ *degree*	α *db*	ε'_r	tan δ x 10^{-4}
1	109.5	0.350	3.40	211.4	79.8	0.440	2.50	288.8	56.0	0.740	1.59	531.8
2	219.5	0.710	3.41	214.3	160.2	0.720	2.50	235.9	114.0	1.130	1.97	404.4
3	328.5	0.940	3.41	189.1	243.9	1.440	2.53	313.2	168.9	0.780	1.96	186.5
4	438.1	1.480	3.40	233.5	324.2	1.570	2.53	256.4	232.5	0.145	2.00	25.8
5	547.6	1.755	3.40	212.1	411.5	2.290	2.56	297.7	286.0	0.185	1.98	26.5
6	657.5	2.110	3.40	212.4	494.6	2.125	2.58	230.1	342.6	0.720	1.97	85.1
7	762.2	2.620	3.38	226.7	582.1	2.440	2.58	225.8	406.0	1.230	1.99	125.2
8	870.7	2.760	3.38	219.0	663.4	1.800	2.58	145.9	464.7	0.410	1.99	36.5
9	979.3	3.270	3.38	220.1	749.1	2.065	2.58	148.6	520.5	0.085	1.99	6.7
10	1089.7	3.630	3.38	219.8	830.0	1.460	2.58	94.6	575.2	0.995	1.99	29.6

Table 1.

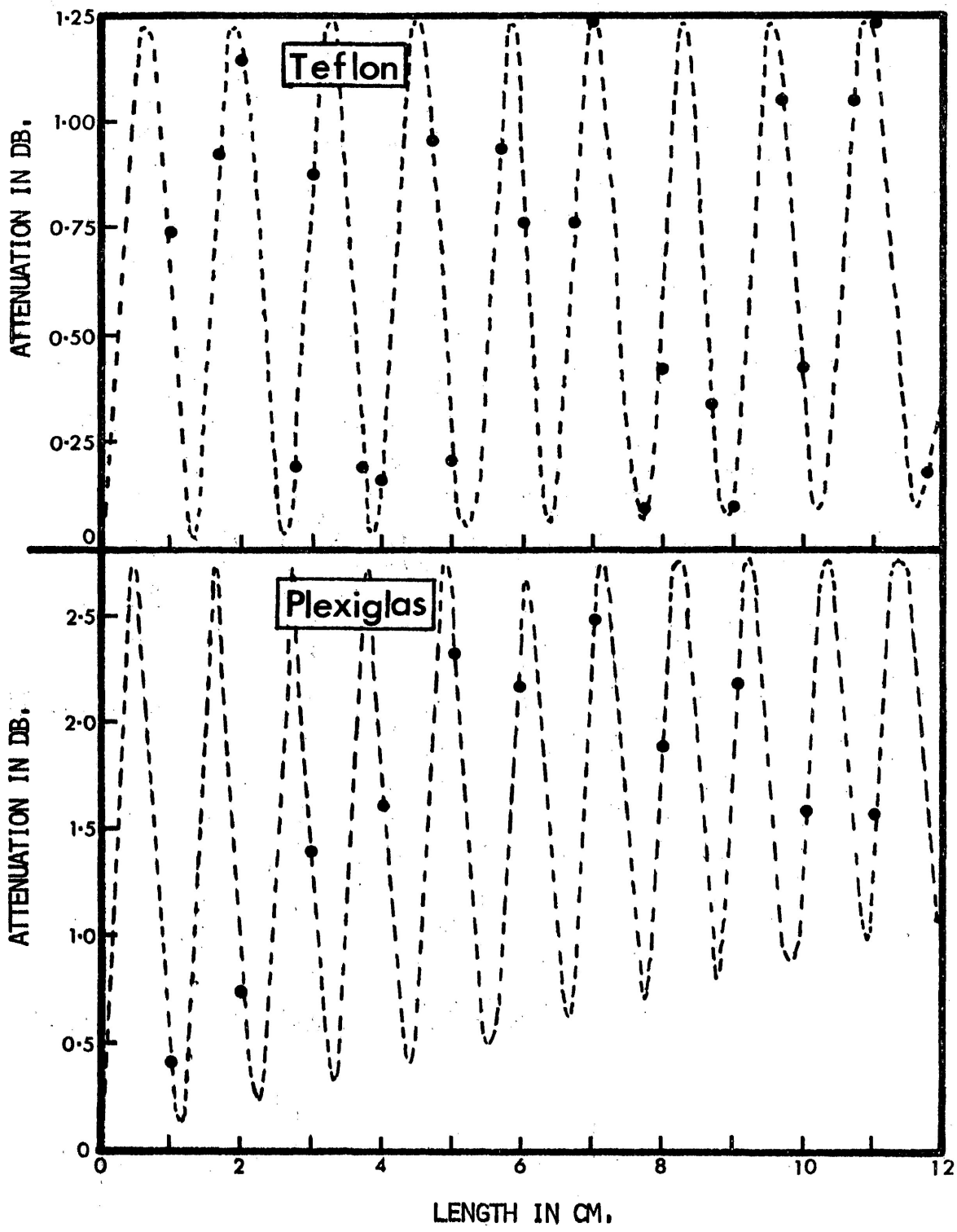

Figure 7. Attenuations of arbitrary lengths of samples of teflon and plexiglas as a function of length.

5. Correction for Low-Loss Materials

(a) Theoretical Improvements

In § 3, The equations for ε_r' and ε_r'' were derived by ignoring R_∞^2 compared to unity, so that (11) would be written in the simple form (13). However, if multiple reflections are to be taken into account, corrections to equations (18) and (19) may be required.

For simplicity, consider very small losses so that R_∞ is practically real, and also $R_\infty^2 << 1$. The objective here is to put (12) into the form

$$T = |T|e^{i\theta} \tag{23}$$

to get the phase shift and attenuation. (12) could be written in the following form,

$$T = \frac{1 - R_\infty^2}{1 - R_\infty^2 e^{2ik'd} e^{-2k''d}} e^{i(k' - k_g)d - k''d} \tag{24}$$

Since $R_\infty^2 << 1$, the first factor may be written as

$$\frac{1 - R_\infty^2}{1 - R_\infty^2 e^{2ik'd - k''d}} \doteq (1 - R_\infty^2)(1 + R_\infty^2 e^{2ik'd - 2k''d})$$

$$\doteq (1 - R_\infty^2)\left[1 + R_\infty^2(\cos 2k'd + i \sin 2k'd)e^{-2k''d}\right]$$

$$\doteq \left[1 - R_\infty^2(1 - e^{-2k''d}\cos 2k'd)\right] + \left[i\, R_\infty^2 e^{-2k''d}\sin 2k'd\right]$$

where terms containing R_∞^4 were dropped. Letting now

$$a = 1 - R_\infty^2(1 - e^{-2k''d}\cos 2k'd)$$

$$b = R_\infty^2 e^{-2k''d}\sin 2k'd$$

the first factor may then be written as

$$a + ib = (a^2 + b^2)^{\frac{1}{2}}\left[\frac{a}{(a^2 + b^2)^{\frac{1}{2}}} + i\frac{b}{(a^2 + b^2)^{\frac{1}{2}}}\right]$$

$$= (a^2 + b^2)^{\frac{1}{2}} \cdot e^{i\beta}$$

where $\tan\beta = \frac{b}{a}$. Since in general $\frac{b}{a}$ is small (because $R_\infty^2 << 1$), the following approximations can be made: $\beta \doteqdot \frac{b}{a} \doteqdot b$, also $(a^2 + b^2)^{\frac{1}{2}} \doteqdot a$ since $a^2 >> b^2$, and the first factor of (23) becomes

$$ae^{ib} = \left[1 - R_\infty^2\,(1 - e^{-2k''d}\cos 2k'd)\right]e^{i(R_\infty^2 e^{-2k''d}\sin 2k'd)}$$

so that (23) becomes

$$|T| = \left[1 - R_\infty^2\,(1 - e^{-2k''d}\cos 2k'd)\right]e^{-k''d} \qquad (25)$$

$$\theta = (k' - k_g)d + R_\infty^2 e^{-2k''d}\sin 2k'd \pm 2n\pi \quad . \qquad (26)$$

The attenuation in db is thus

$$\alpha = -20\log_{10}|T|$$

$$= 8.686k''d - 8.686\,ln\left[1 - R_\infty^2\,(1 - e^{-2k''d}\cos 2k'd)\right]$$

$$\alpha \doteqdot 8.686\left[k''d + R_\infty^2(1 - e^{-2k''d}\cos 2k'd\ )\right] . \qquad (27)$$

The results (26) and (27) should replace (14) as a better approximation when R_∞^2 is taken into account. However, it is now difficult to solve for k' and k'' explicitly in order to find ε_r' and ε_r''.

Having regard to the assumption of small losses, however, one may replace $e^{-2k''d}$ by 1 in (26) and (27) to give

$$\theta \doteqdot (k' - k_g)d + R_\infty^2 \sin 2k'd \pm 2n\pi \qquad (28)$$

$$\alpha \doteqdot 8.686k''d + 17.372\ R_\infty^2 \sin^2 k'd \qquad (29)$$

Now if (18) is regarded as a first approximation to ε_r', it is clear that in low-loss dielectrics the middle term is negligible compared to the other two terms, in which case

$$\varepsilon_r' \doteqdot \left[\frac{\lambda_o(\theta \pm 2n\pi)}{2\pi d} + \frac{\lambda_o}{\lambda_g}\right]^2 + \left(\frac{\lambda_o}{\lambda_c}\right)^2 . \qquad (30)$$

Since

$$\lambda \doteqdot \frac{\lambda_o}{\sqrt{\varepsilon_r' - \left(\frac{\lambda_o}{\lambda_c}\right)^2}} \qquad (31)$$

is the wavelength inside the dielectric, this and (30) give

$$k' = \frac{\theta \pm 2n\pi}{d} + \frac{2\pi}{\lambda_g} \qquad (32)$$

Substituting (32) into (28) and (29) gives

$$\theta \doteqdot (k' - k_g)d + R_\infty^2 \sin 2(\theta + \frac{2\pi d}{\lambda_g}) \pm 2n\pi$$

$$\alpha \doteqdot 8.686k''d + 17.372\, R_\infty^2 \left[\sin^2(\theta + \frac{2\pi d}{\lambda_g})\right] . \qquad (33)$$

From these we have

$$\frac{k'}{k_o} = \frac{\theta \pm 2n\pi - R_\infty^2 \sin 2(\theta + \frac{2\pi d}{\lambda_g})}{k_o d} + \frac{k_g}{k_o} \qquad (34)$$

$$\frac{k''}{k_o} = \frac{\alpha - 17.372\, R_\infty^2 \sin^2(\theta + \frac{2\pi d}{\lambda_g})}{8.686 k_o d} . \qquad (35)$$

The equation of ε_r' and ε_r'' in § 3 could be rewritten as

$$\varepsilon_r' = (\frac{k'}{k_o})^2 - (\frac{k''}{k_o})^2 + (\frac{\lambda_o}{\lambda_c})^2 \qquad (36)$$

$$\varepsilon_r'' = 2(\frac{k'}{k_o})\ (\frac{k''}{k_o}) . \qquad (37)$$

By substituting (34) and (35) into (36) and (37), the second approximation to the dielectric constant and loss is thus

$$\varepsilon_r' = \left[\frac{\theta \pm 2n\pi - R_\infty^2 \sin 2(\theta + \frac{2\pi d}{\lambda_g})}{k_o d} + \frac{k_g}{k_o}\right]^2 - \left[\frac{\alpha - 17.372 R_\infty^2 \sin^2(\theta + \frac{2\pi d}{\lambda_g})}{8.686\, k_o d}\right]^2 + \left(\frac{\lambda_o}{\lambda_c}\right)^2 \tag{38}$$

$$\varepsilon_r'' = 2\left[\frac{\theta \pm 2n\pi - R_\infty^2 \sin 2(\theta + \frac{2\pi d}{\lambda_g})}{k_o d} + \frac{k_g}{k_o}\right] \times \left[\frac{\alpha - 17.372 R_\infty^2 \sin^2(\theta + \frac{2\pi d}{\lambda_g})}{8.686\, k_o d}\right] \tag{39}$$

It is now interesting to note that (38) and (39) differ from (18) and (19) only by R_∞^2 terms, and that the effect of R_∞^2 in (39) is to lower the dielectric loss from the value obtained by ignoring this correction. However, although (38) and (39) are helpful, they are tedious to use in calculations.

Furthermore, some approximations have already been made in their derivation. Fortunately an experimental correction, discussed below, can be made which precludes the necessity of using them.

(b) Experimental Improvements

The propagation constant k inside the dielectric contains an attenuation constant k'' and a phase constant k'. The phase constant represents the number of radians of phase shift per unit length of line, while the wavelength λ is the distance required for a phase shift of 2π radians, hence $k' = 2\pi/\lambda$. For very low losses this term dominates and thus can be substituted for k in the denominator of (23). Therefore, for very low losses;

$$T \doteqdot \frac{1 - R_\infty^2}{1 - R_\infty^2 \, e^{2i\frac{2\pi}{\lambda} d}} \; e^{i(k' - k_g)d - k''d}$$

and it can be seen that if we select $d = \frac{n\lambda}{2}$, then

$$T = e^{i(k' - k_g)d - k''d} \tag{40}$$

But (40) has the same form as (13) which was obtained by ignoring the R_∞^2 terms of (12). In other words, (18) and (19) could still be used again for low-loss dielectric provided that the sample is cut to multiples of half-wavelength inside

the dielectric. This result simply means a sample length of exactly multiple-halfwavelengths would eliminate the multiple reflections inside the dielectric which were formerly ignored by using the approximate formula (13).

6. Additional Measurements and Results

To find the wavelengths inside the dielectrics, the results obtained by our preliminary measurements, § 4, for the dielectric constant ε_r' was used in (31). Samples of ertalon, teflon and plexiglas were then cut into different multiples of half-wavelengths, respectively to an accuracy of ± 0.001".

Before repeating the measurements, it was noticed that the lengths of the samples may not be precise enought for this experiment due to the fact that when R is close to zero (at the half-wave points) there is a cusp and thus a very minute change of d may cause appreciable reflection. For this reason a fine adjustment to give minimum reflection was thus made by tuning the klystron carefully to obtain a minimum reading of the V.S.W.R. indicator used in conjunction with the slotted line (see Fig. 1). It may be argued that this change of frequency would effect the value of dielectric constant. Nevertheless, the change would be very small. As a matter of fact, the Kramers-Kronig Dispersion Relation:

$$\varepsilon'(\omega) - 1 = \frac{2}{\pi}\int_0^\infty \frac{\omega'\varepsilon''(\omega')d\omega'}{\omega'^2 - \omega^2} \tag{41}$$

predicts that the lower the loss of the dielectric, the less is the sensitivity of ε' to frequency. The new working frequency was noted and the measurements were made again by following the same procedure as in § 4.

7. Conclusions and Discussion

A comparison of the first set of data (Table 1) with the new set (Table 2) for ertalon shows that the results are very close to each other. The small decrease in α in the second set of results indicates the effect of small multiple-reflection of the signal due to the sample. Nevertheless, the reflection coefficient R_∞ is small enough and the loss high enough to ensure the simple formula, (13) will apply in good approximation.

It has been mentioned in Section 4, in the case of teflon and plexiglas, the attenuation fluctuated with minima occurring at regular intervals of length. Careful inspection of these graphs showed that, to a close approximation, the regular intervals equal half the wavelength calculated by using (31). Furthermore, for samples which are multiples of half-wavelengths, plots of α *versus* sample length are not only linear (Fig. 8), but found to touch the minima of the former graphs (Fig. 7) in each case. This observation substantiates the use of half-wavelength samples.

One may well wonder if the simpliest way to do the experiment is to adjust the klystron frequency to get a minimum reading of V.S.W.R. for arbitrary lengths of samples. It should be noticed, however, that the klystron is adjusted for optimum output for the desired mode of operation and extensive de-tuning is thus

Additional Measurements of Dielectric Properties of:

Ertalon					Plexiglas					Teflon				
Frequency = 9.16 GHz					Frequency = 9.54 GHz					Frequency = 9.54 GHz				
d	θ	α	ε_r'	$\tan\delta$ x 10^{-4}	d	θ	α	ε_r'	$\tan\delta$ x 10^{-4}	d	θ	α	ε_r'	$\tan\delta$ x 10^{-4}
0.97	104.0	0.32	3.37	200.0	1.09	89.5	0.100	2.56	59.7	1.28	73.7	0.006	1.99	3.4
1.94	209.5	0.62	3.34	193.2	2.18	179.4	0.190	2.56	56.7	2.56	148.1	0.013	1.99	3.6
2.91	318.5	0.90	3.38	185.9	3.27	267.9	0.280	2.56	55.8	3.38	223.9	0.022	2.00	4.1
3.88	420.5	1.33	3.35	206.9	4.37	357.8	0.387	2.56	57.8	5.11	298.5	0.025	2.00	3.5
4.85	530.7	1.55	3.38	192.2	5.45	449.1	0.490	2.57	58.5	6.39	378.3	0.030	2.02	3.3
5.82	632.6	1.90	3.36	196.8	6.53	536.5	0.650	2.56	64.7	7.67	452.9	0.045	2.02	4.2
6.97	741.5	2.21	3.37	195.9	7.62	628.3	0.750	2.56	64.0	8.95	522.9	0.053	2.01	4.2
7.76	847.5	2.58	3.37	200.1	8.71	716.0	0.850	2.56	63.5	10.22	608.5	0.053	2.03	3.7
8.73	954.3	2.80	3.38	192.9	9.80	807.0	0.960	2.56	63.7	11.50	688.3	0.055	2.03	3.4
9.70	1061.5	3.18	3.38	197.1	10.89	896.0	1.040	2.56	62.1	12.78	751.9	0.074	2.01	4.1

Table 2.

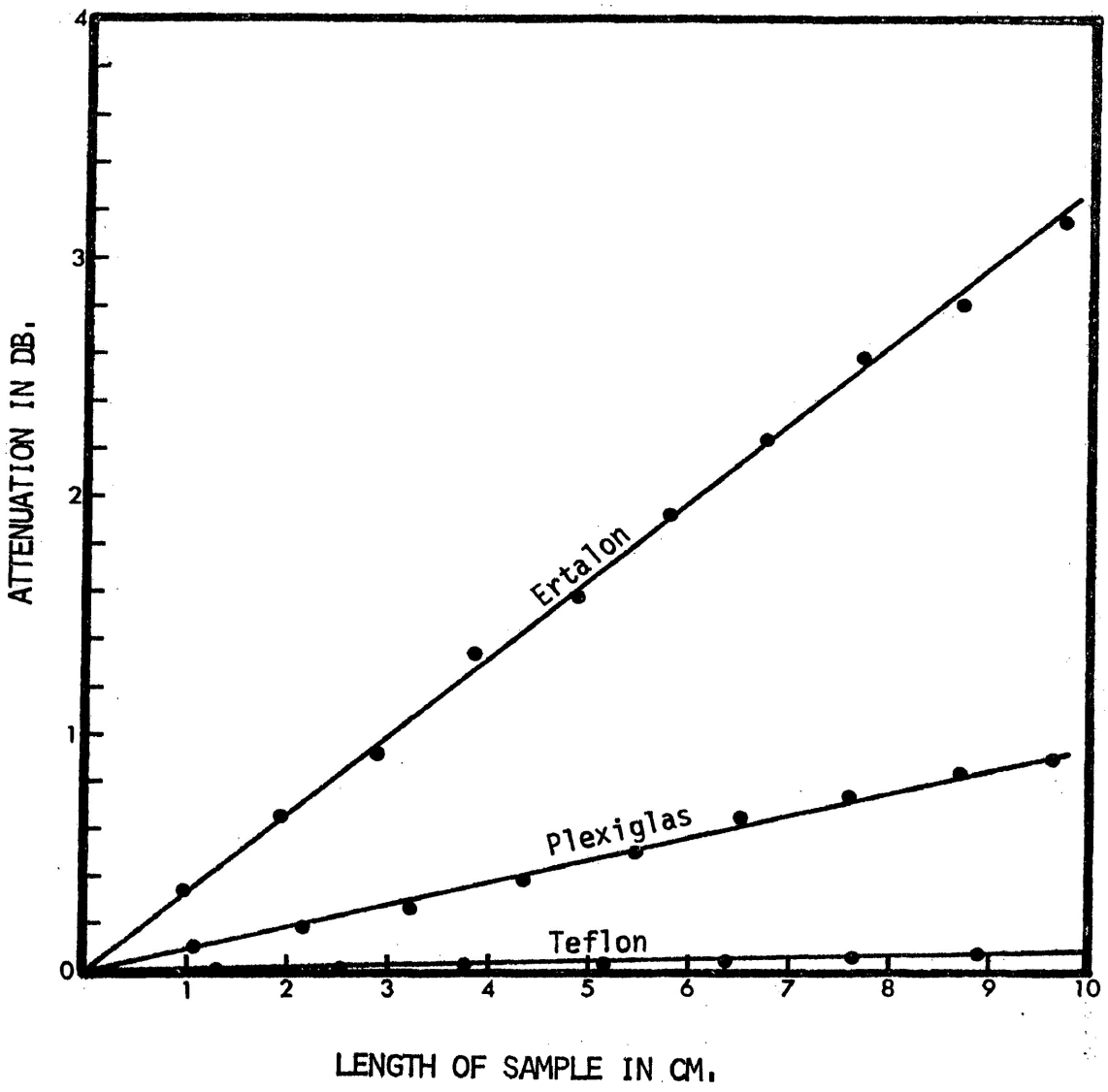

Figure 8. Attenuations of integral half-wavelength samples as a function of length.

not advisable. Furthermore, the frequency range of the klystron may not be wide enough to cover the minimum V.S.W.R. necessary to give a half-wavelength in a given sample. The following table gives a range of frequencies to insure half-wavelengths in teflon samples with lengths between 2 and 3 cm.

LENGTH IN CM.	2.0	2.1	2.2	2.3	2.4	2.5	2.6	2.7	2.8	2.9	3.0
OPTIMUM FREQUENCY (GH_z)	11.577	11.161	10.701	10.324	9.983	9.671	9.386	9.125	8.884	8.662	8.457

Table 3.

As a final remark, it may be mentioned that the present system, could be improved both electrically and mechanically. Suggestions include the used of a more powerful klystron, a more precise attenuator and phase shifter. The system could also be extended to other frequency bands of the microwave region.

PART 2

Application of the System: Dielectric Constants and Losses of Polystyrene and Dilute Solutions of Polar Molecules in Polystyrene.

8. Introduction

(a) Structure of Pure Polystyrene

As an application of the system to media of unknown ϵ_r , the dielectric properties of polystyrene was investigated. Polystyrene is one of the oldest synthetic materials known. Because of its many desirable properties, it is now one of the most important thermoplastic materials. Although it has been studied for a great many years, much concerning its detailed behavior is yet to be discovered.

The object of this part of the thesis is to study the temperature dependence of the dielectric constant and dissipation factor of pure polystyrene and polystyrene doped with dilute amount of polar impurities. The polystyrene molecule $(CH_2CHC_6H_5)_n$ has the repeating structure shown in Figure 9. The four bonds of the C-atom in the CH_2 or CH group form the vertices of a regular tetrahedron. In view of the interaction between the atoms, the distribution of electrons in the molecule should be axially symmetrical around the line joining the nuclei of the two atoms. In this case, the C-H bonds will have a dipole moment while the C-C bond should have no moment for reasons of symmetry.

The direction of dipole moment would be discussed based on the assumption that all four bonds of a C-atom make tetrahedral angles of $\theta=2\cos^{-1}(1/\sqrt{3})=109^{o}$ with each other . The resultant diople moment is then always in the C-C-C plane(Figure 10) besecting the C-C-C angle as shown by Fröhlich(1958). The dipole moments of the C-H groups in the benzene ring cancel one another due to the hexagonal symmetry, except the one which is in the direction of the adjoining C-C bonds. A resultant moment

is thus formed by the C-benzene group in exactly opposite direction to the former one as shown. Assuming all the C-H dipoles are equal, the dipole moment of each subgroup and hence of the whole molecule vanished exactly.

To be more complete, the structure at the end of the polymer chain is also considered. When the polymer chain ends there will be a remaining bond from the C-atom which forms an end group with some other molecule or atom. This end group varies with different kinds of polymerization and initiators used. In the simpliest case, a C-H bond will be formed at each end by acquiring an additional H atom. The contribution of dipole moment of the end groups depends on their concentration in the polymer. Since polystyrene has a high molecular weight(of about 230,000) the concentration of the end groups is so small that their contribution to the dipole moment of the whole molecule is negligible. The molecule is therefore regarded as essentially non-polar.

At room temperature pure polystyrene is a hard, amorphous, glassy solid; above 85°--100°C it becomes more flexible. The temperature at which it softens is known as the glass-transition point. In this experiment, due to technical limitations, only the dielectric behavior of polystyrene below the glass-transition temperature was studied.

(b) Polar Impurities in Polystyrene

The study of polar impurities in polystyrene is also the subject of interest. Here a dilute solution of a polar material called 8-Quinolinol or 8-Hydroxyquinoline(C_9C_6NOH) was used in polystyrene in

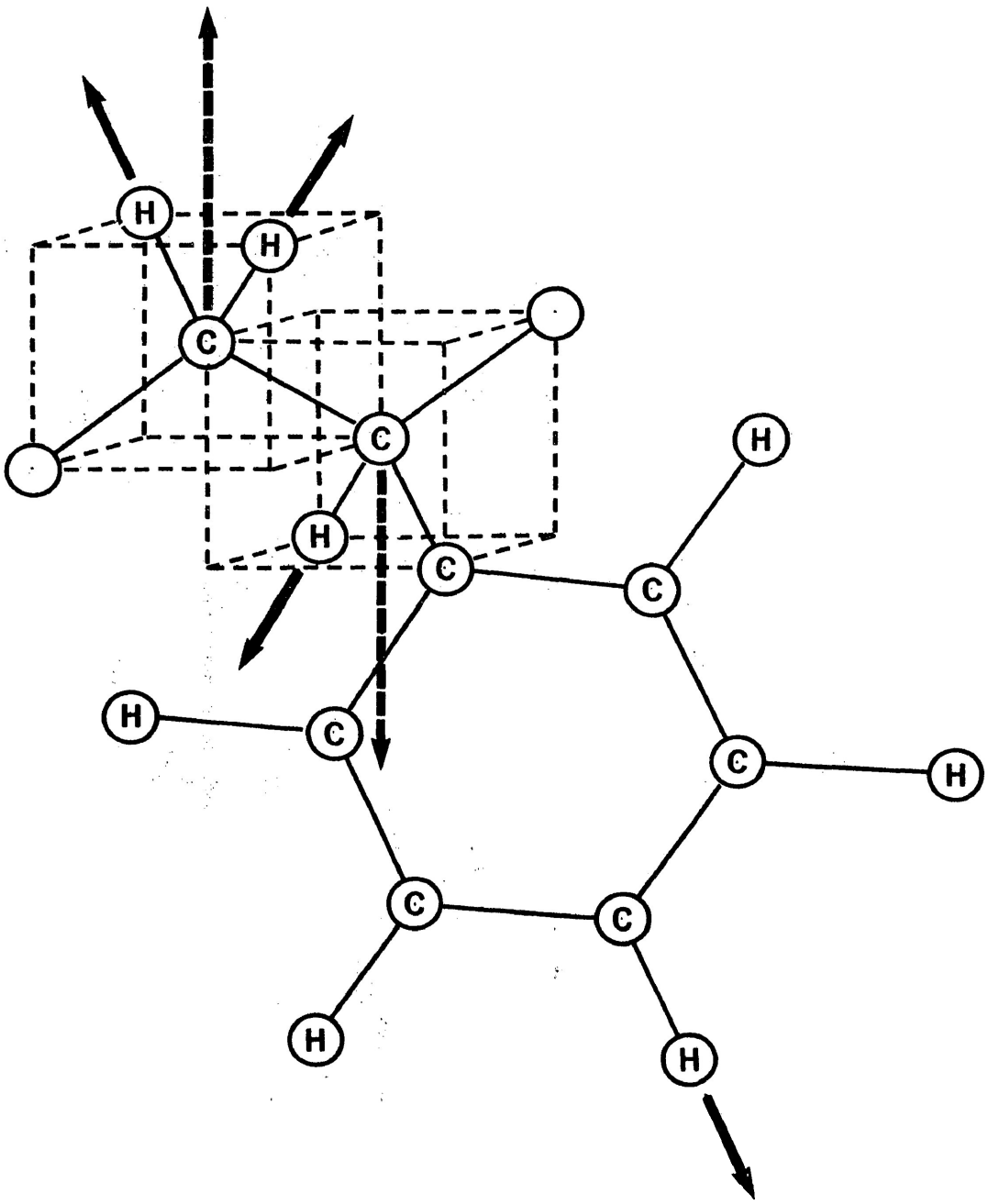

Figure 9. Molecular Structure of Polystyrene. Solid and dotted arrows respresent dipole moments and resultant diople moments respectively.

several proportions by weight; viz, 0.1%, 0.4%, 0.8%, 1%, 1.4%, 1.8% and 2%. 8-Quinolinol is interstitial in solid polystyrene and has the stable molecular structure shown in Figure 10. Here the O-H bond forms a dipole moment in the direction shown while the O-Benzene bond forms another dipole in the vertical direction. The resultant dipole is represented by the dashed arrow. The dashed line in the figure is the weak bond joining the hydrogen atom of the O-H group and the lone pair of electrons from the nitrogen atom.

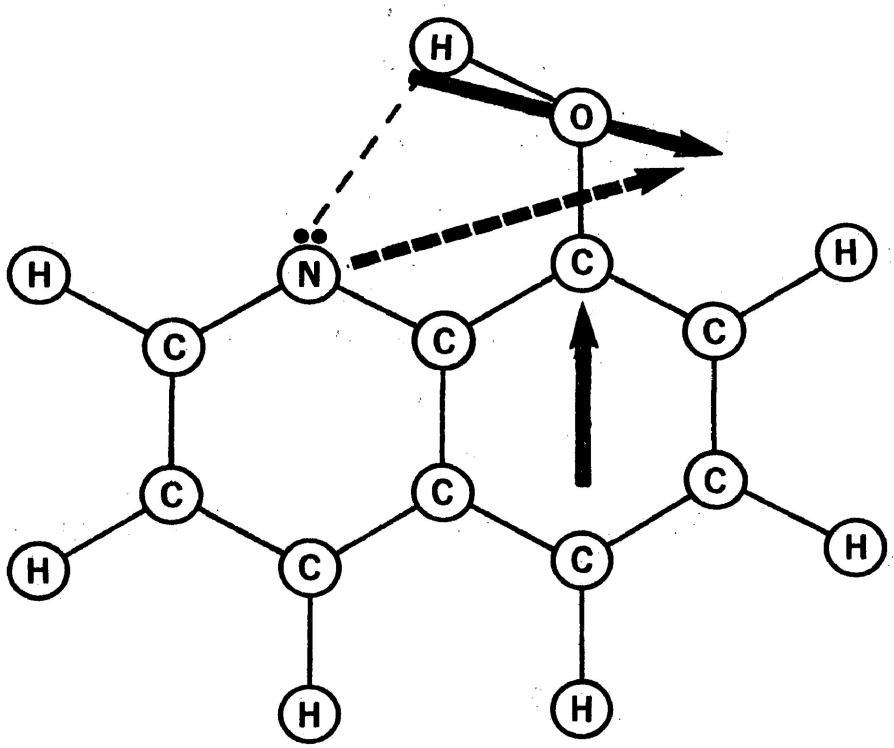

Figure 10. Stable molecular structure of 8-hydroxyquinoline. Solid arrows are the dipole moments of the individual groups while the dashed arrow is the net dipole of the molecule.

Since the potential barrier of this weak bond is very low (about 4kcl/mole), it can easily be broken upon thermal agitation. A new configuration is thus formed as the O-H bond rotates around the O-C axis. This intramolecular process(i.e., the rotation of the O-H bond) changes the direction of the O-H dipole. As a result, the direction of the resultant dipole also changes as shown in Figure 11. This configuration, however, is very unstable because of the interaction between the H atom of the O-H group and the nearest H atom. The net dipole moment of 8-Quinolinol is 1.68-2.68 Debye units at 25°C, according to the Tables of Experimental Dipole Moments by McClellan(1963).

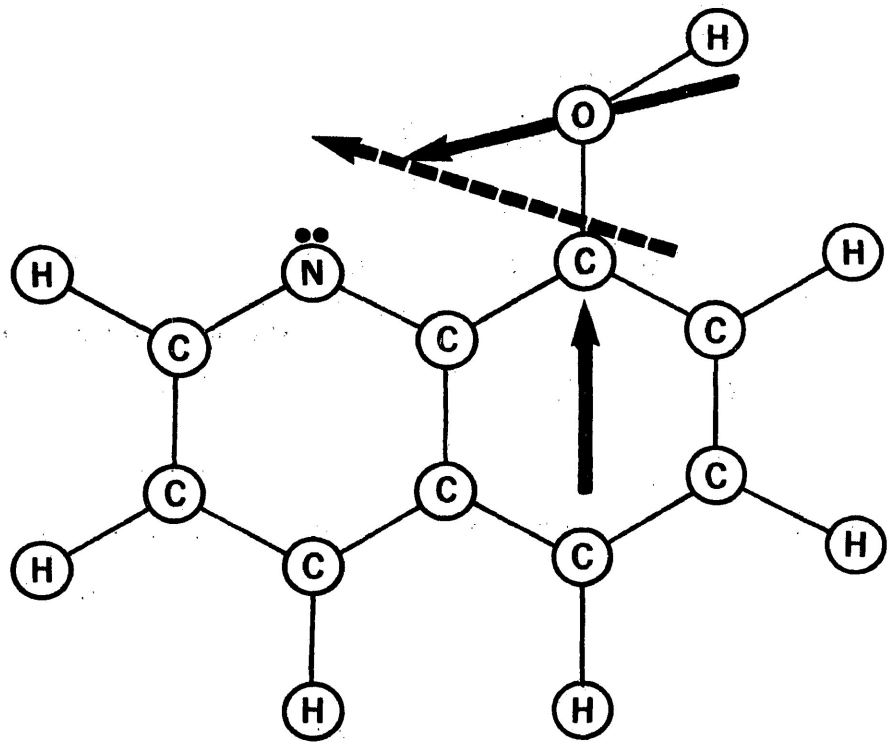

Figure 11. Unstable molecular structure of 8-Quinolinol.

As previously explained, pure polystyrene behaves like a non-polar solvent in the liquid state,but when a dilute amount of polar substance(8-Quinolinol,in this case) is added, the effect of the orientational polarization of the polar solute is observed.

Dichloroethylene(ClCH:CHCH), a flammable organic solvent was used here to dissolve polystyrene fragments and 8-Quinolinol powders during the preparation of samples. The former substance is a non-polar solution, so that the very small residual amount remaining in the sample could not contribute appreciably to the measured dielectric properties.

9. Preparation of Polystyrene Samples

The polystyrene in this experiment was initially in fragment form. In order to make suitable samples, the following procedure was used:

(1) Pure Polystyrene

Twenty-five gm. of polystyrene were weighed in a precision balance (accurate to one-thousands of a gram), and then poured into a 2-inch diameter die which was surrounded by a heated coil. The temperature of the coil was controlled by a thermocouple to maintain it at about 115^{o}C. The content was heated until soft enough(about 20 minutes) to be compressed by a hydraulic press. A pressure of about ½ ton was first applied and then released. This was repeated two or three times to enable the air bubbles to escape from inside the material. Finally, a pressure of about 8 tons was applied for about 15 seconds which gave a disk of ½ inch thickness. A good sample should be free of air bubbles and transparent.

(2) Doped Polystyrene

Appropriate proportions of polystyrene fragments and 8-Quinolinol powders were weighed, respectively, to give a total of 25 gm. They were mixed and then dissolved in 1,2-Dichloroethylene solution. The content was then heated in an oven to about 115^{o}C. While in the oven, the solute dissolves gradually as the solvent evaporates. About 25 minutes later, the content became a paste which dried out eventually.

The mixture was then transferred to another oven which was equiped with a vacuum pump. While the material was being heated and evacuated, it foamed and became sponge like. This step took about 15 minutes to ensure that all the air bubbles were evacuated and that more than 99% of the solvent was dried out--as was latter checked by re-weighing the material. This compound was then ready to be compressed as described in (1) above. The polystyrene was never heated to more than 115∿135^{o}C so that the sample did not oxidize.

(3) Machining the samples into the waveguide dimensions was mainly done using a milling machine. Before proceeding, it was noticed that the accuracy of the results of measurements depend to a large extent on the smoothness of the sample, accurate fitting of the sample in the waveguide, and the care which has been taken to ensure that its surfaces are properly "square" with respect to each other. It was noticed that the smaller the sample the more critically the experiment will depend upon sample irregularity. Therefore,the samples were machined carefully for smoothness, size and square surfaces.

Experiences by other experimentalists such as Wind and Rapaport (1955), show that a slide fit, at least, should be specified in designing the dielectric sample for insertion into the waveguide; however, a force fit is preferable. Also it was suggested that the only correction needed for samples in rectangular waveguide are for those with air space parallel to the "a" dimension(Figure 12). Similar air space parallel to the "b" dimension would give rise to only negligible

measurement error in view of the vanishing electric field component at the side walls of the waveguide. Because the samples have to be interchanged from time to time during the experiment, they were all made with thichness exactly equal to the "b" dimension, while slide fits were given to the side walls; i.e., the "a" dimension.

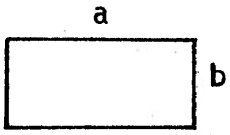

Figure 12. Inner dimensions of waveguide; a=0.9" and b=0.4".

10. Temperature Behavior of Sample Holder

Before proceeding with the experiment, it was noted that the effect of temperature on the waveguide should not be neglected. Hence the change of phase shift and attenuation due to the rise of temperature in the bare waveguide sample holder was first studied. It was found that within the temperature range(20°-80°C) the phase shift due to the empty waveguide decreases almost linearly with temperature while the attenuation remains unchanged within experimental error. A plot of the respective characteristics is given in the following Figure.

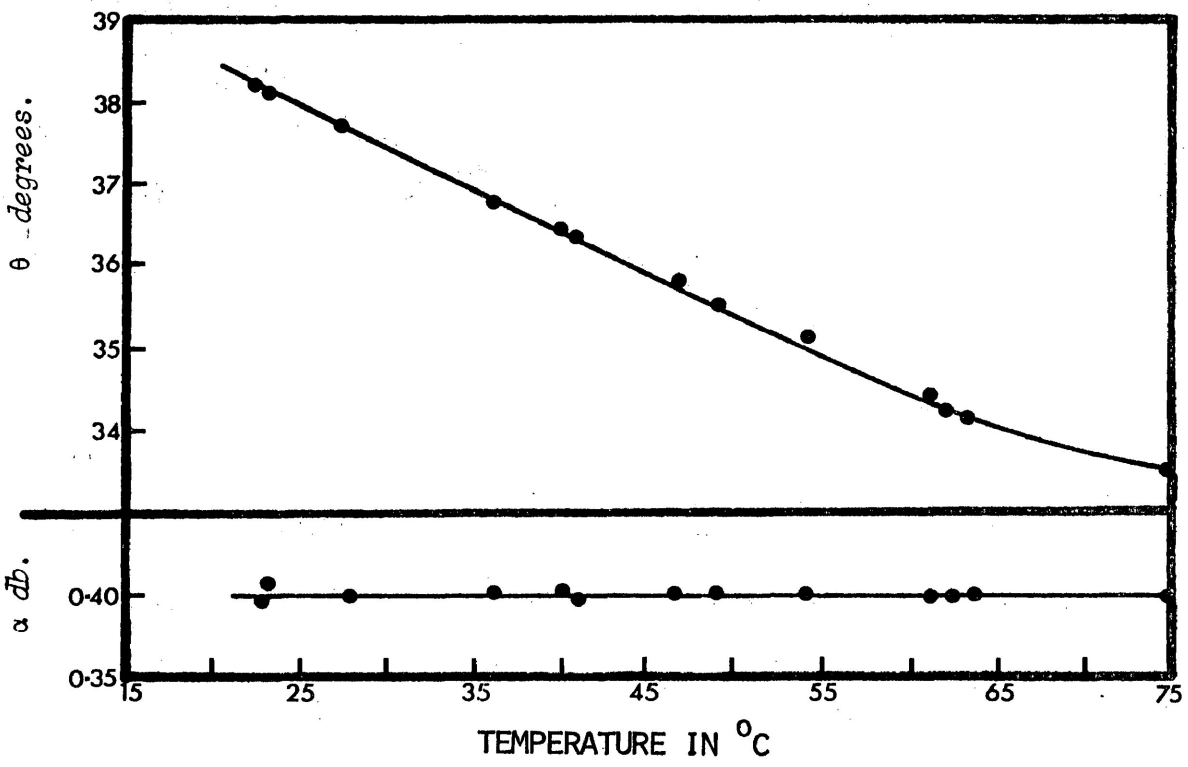

Figure 13. Temperature dependence of sample holder.

Subsequent measurements of α and θ for samples at different temperatures were base on these two curves as "zero point" readings.

Since the temperature in the sample section of the waveguide was not completely uniform, the readings at the same temperature varied if the waveguide was heated for different lengths of time. In order to minimize this deficiency, the same procedure was carried out to maintain consistancy as far as possible. The variable transformer was first set to 60 division which would give an upper temperature of 75°C in about an hour. After one hour time the setting of the transformer was decreased by 10 divisions and was further decreased by 10 divisions at every half-hour until it was off. During this time, the temperature of the waveguide dropped steadily and returned to room temperarure at about an hour after the zero division was set. Readings could very well be taken even when the temperature first showed signs of dropping since the bridge could always be balanced due to the long thermal time constant.

11. Results of Dielectric Measurements

(a) Polystyrene

Samples of arbitrary lengths were first measured at room temperature. As in Part 1, it was found that for arbitrary lengths the phase shift and attenuation were non-linear and fluctuating with length. When half-wavelength samples were used the attenuation became linear again(see App. A and B). A similar relationship of attenuations exists between the two measurements; i.e., the second curve touches the minima of the first curve as shown in Figure 14.

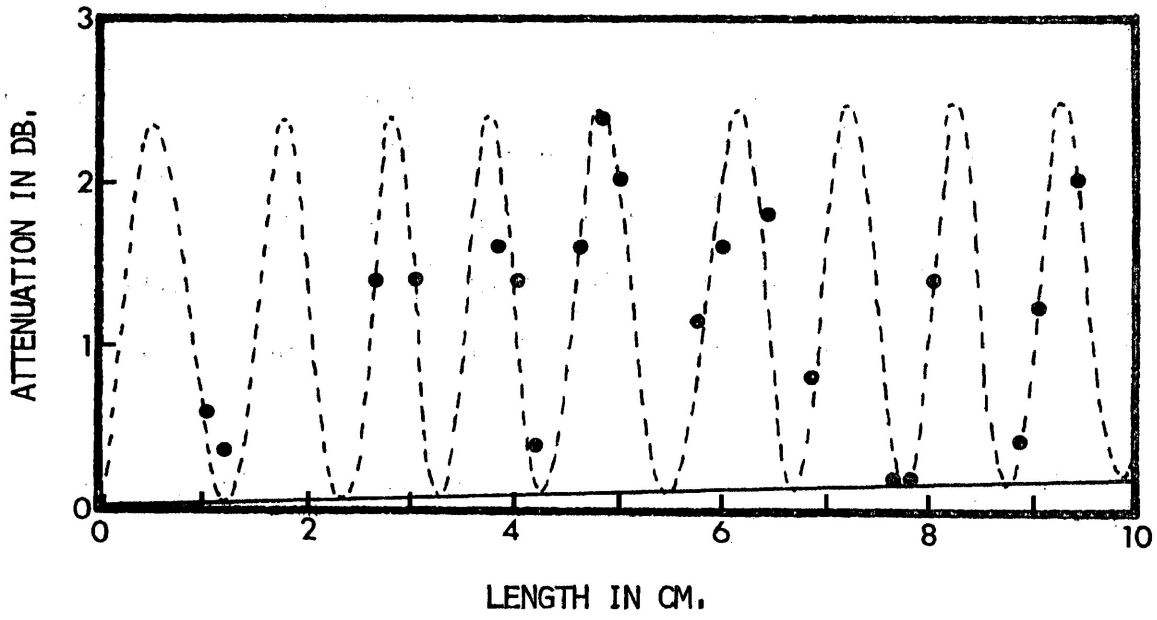

Figure 14. Attunation of pure polystyrene as a function of length. The solid curve is the result obtained by using half-wavelength samples.

Previous research has shown that for non-polar materials(i.e. molecules with no net permanent dipole moment) the dielectric constant is due to the electronic polarization only. Since electronic polarization is nearly instantaneous the dielectric constant is independent of frequency except in the optical region. Apart from thermal expansion, it is also almost independent of temperature. Losses are thus small at sub-optical frequencies at all temperatures(Appendix C).

At room temperature, polystyrene was found to have a dielectric constant of 2.53±2.8% and a loss tangent of $(3.1\pm9\%)\times10^{-4}$, these figures are extremely close to those published by Von Hippel(1954). As temperature rises, there is a small change to the results, as can be seen in Figures 15 and 16. The small decrease in ε_r' could be accounted for by the decrease in density of the solid as it undergoes thermal expansion. At the same time, the polymer chain segment has more tendency to undergo rotation and bending by acquiring heat as activation energy, thus indicating that ε_r'' should increase with temperature as shown in Figure 16. Although very insignificant below the glass transition point, these changes may cause slight dissipation as temperature rises. Great care has been taken during preparation and with the handling of samples, but there is no guarantee that the sample is completely free of impurities. As stated by Von Hippel(1954), the foreign, non-hydrocarbon group has been found in commercial polystyrene where a similar situation exists. Determination of the oxygen content of various polymers show values that are quite high, of the order of 0.5%. It has been shown that when polystyrene is heated to 100°C in vaccuo, the initial products of decomposition are

mostly water, carbon dioxide, various alcohols, and hydrogen. Such products probably derive from the decomposition of oxygen-containing groups in the polymer formed during polymerization or storage. Consequently, it is believed that the weak losses are caused partly by such foreign groups in the otherwise pure polystyrene.

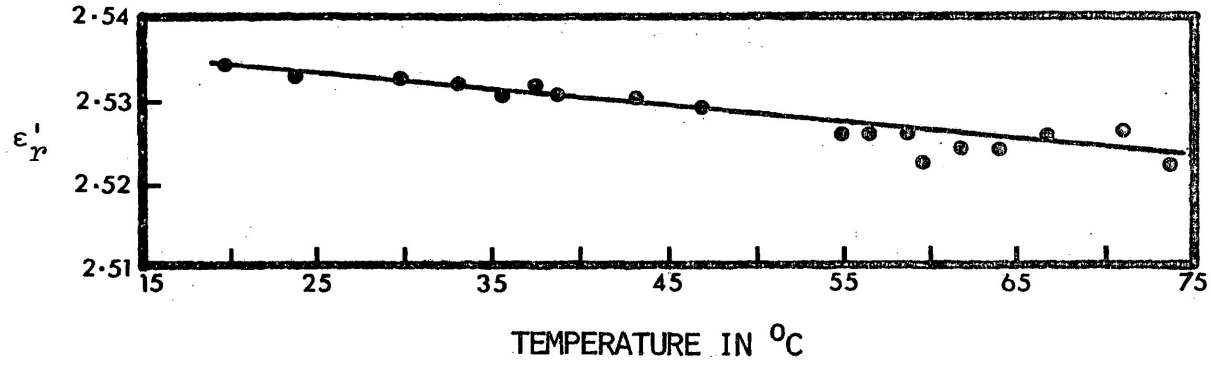

Figure 15. Dielectric constant of pure polystyrene as a function of temperature at f=9.217 GHz.

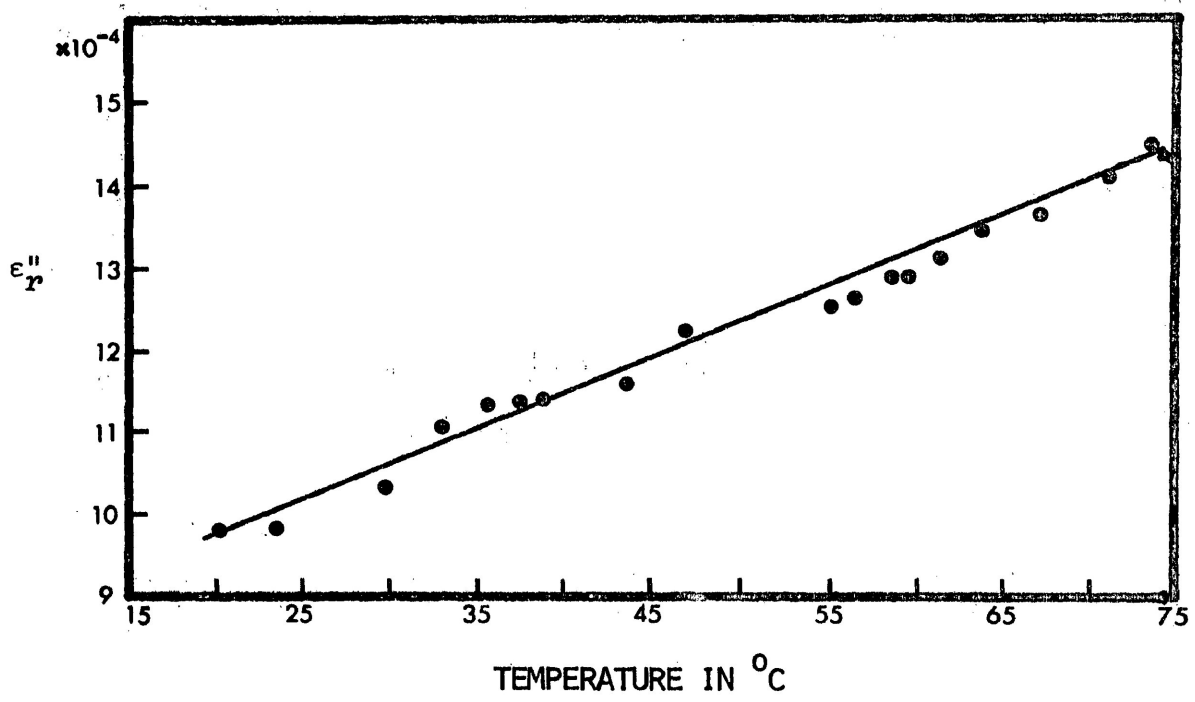

Figure 16 Loss factor of pure polystyrene as a function of temperature at f=9.217 GHz.

(b) Polystyrene weakly doped with 8-Quinolinol

Only one circular disk for each concentration of 8-Quinolinol in polystyrene was made. Each disk could be cut, within geometric limitations, to give one 1½-wavelength sample and two 1-cm samples. Assuming these to be homogeneous, the present system should give valid results,and had a variety of lengths been available, the attenuation is expected to be linear with the length. In this case, one 1½-wavelength sample for each concentration would be necessary; and the two 1-cm samples could be used for the preliminary measurements.

The dielectric behavior of polar plastics is determined largely by dipole orientations. Symth(1955) states that, in general the dielectric constants of polar polymers increase as the concentration of the polar groups increase. Figure 17 illustrates this point for polystyrene. It can also be noticed from Figure 18 and 19 that the polar materials are more likely to be affected by temperature. The data from which Figures 17, 18 and 19 were drawn can be found in Appendices D to J.

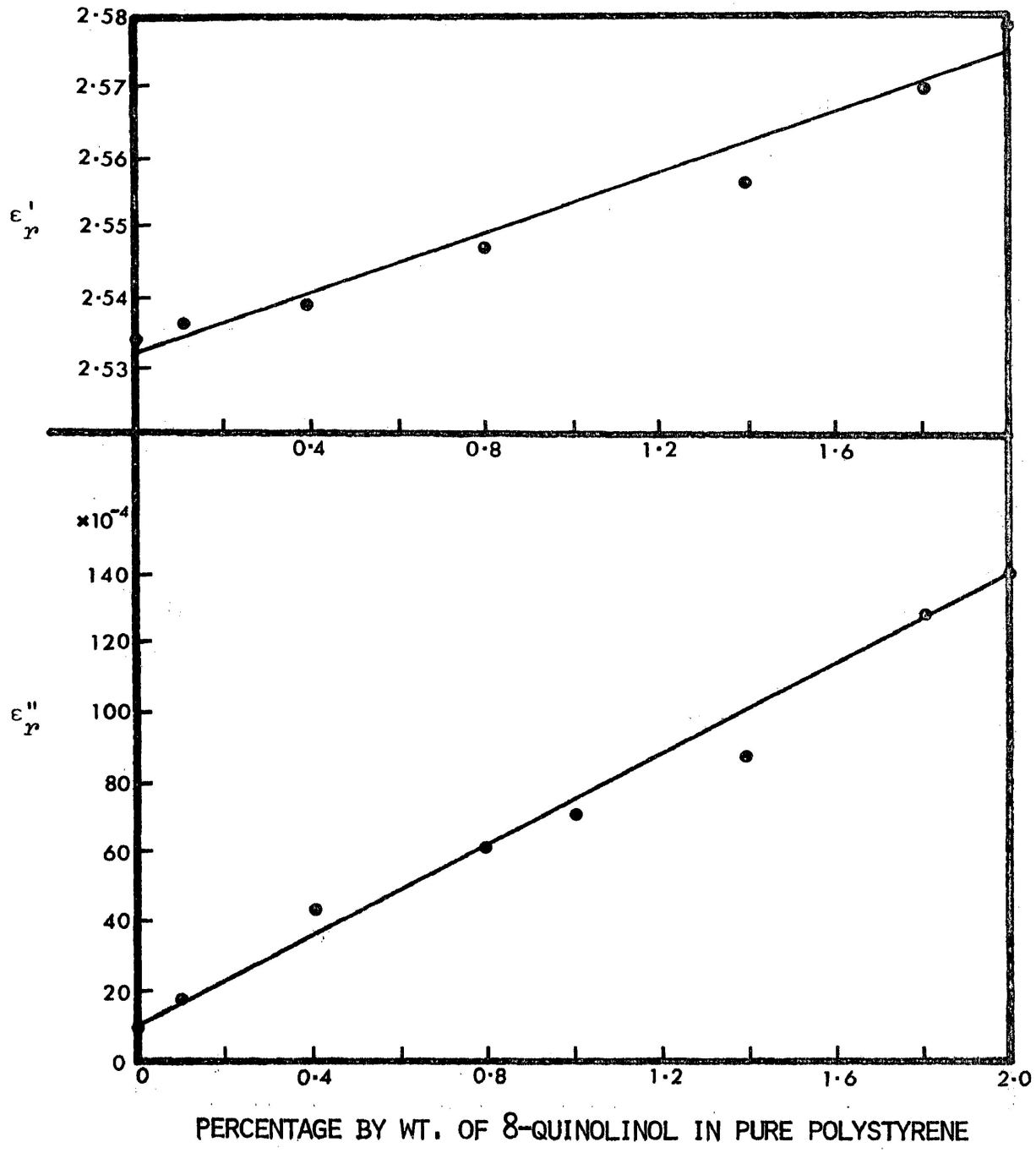

Figure 17. Effect of polar material in non-polar polystyrene at room temperature and f=9.217 GHz.

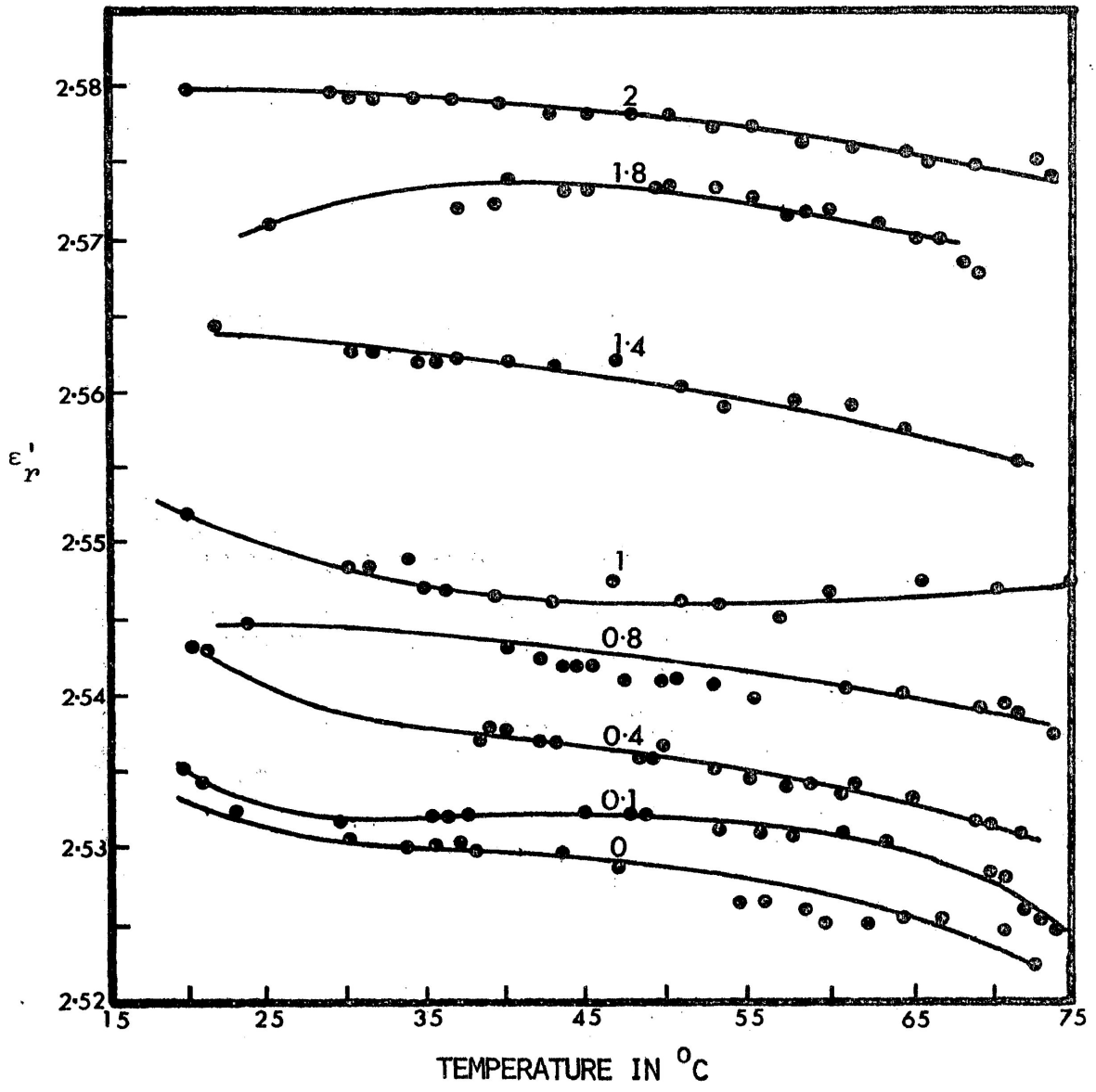

Figure 18. Dielectric constant of doped polystyrene as a function of temperature at f=9.217 GHz. The number on each curve represents the percentage by weight of 8-Quinolinol.

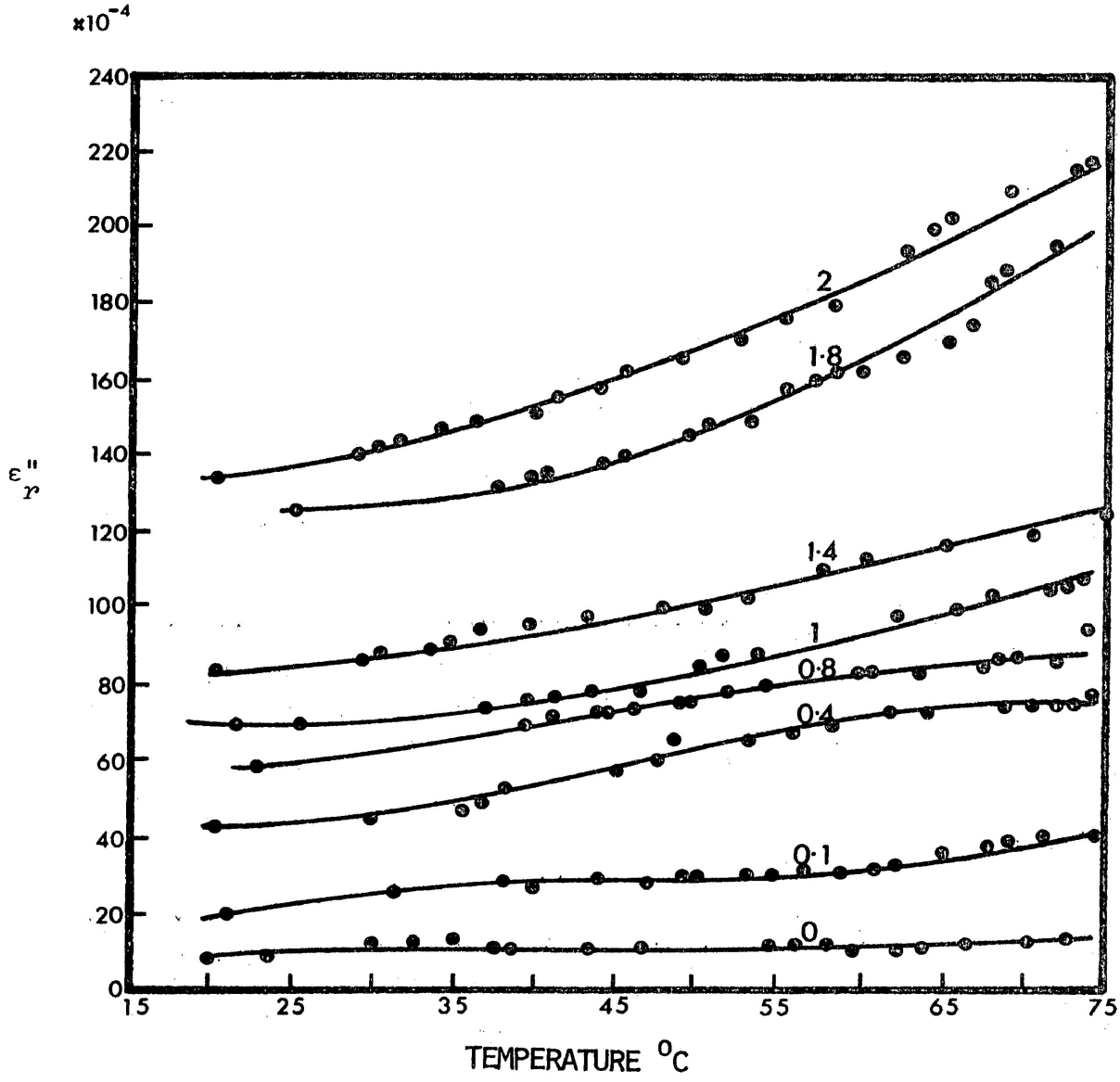

Figure 19. Loss factor of doped polystyrene as a function of temperature at f=9.217 GHz. The number on each curve represents the percentage by weight of 8-Quinolinol.

12. Discussion and Summary

In Part 1 of this thesis a precision method of measuring the permittivity of low-loss solids at microwave frequencies has been described and tested at X - band using materials with known dielectric properties. Although the literature on microwave measurements is extensive, to the best of our knowledge our technique of using the interferometer in the manner discussed here (Part 1) may be new.

It may be remarked that once the preliminary measurement of ε_r' has been made using samples of arbitrary length, the slabs could be cut to the Brewster angle compliment, $\pi/2 - \theta_B$, ($\theta_B = \tan^{-1} \sqrt{\varepsilon_r'}$ = Brewster angle); so that the reflection coefficient of samples with arbitrary lengths would be reduced to small values thereby affording accurate secondary measurements of ε_r' and ε_r''. Since the linearity of α (and θ) with length must be established whichever method is used; the question is one of convenience; viz.: Is it easier to mill samples of arbitrary length to a given angle or to cut square samples to a given length ($n\ \lambda/2$)? With our facilities, the latter was the simpler procedure.

A more serious objection can be raised with respect to temperature measurements. Since the heat bath lacked thermostatic control and the temperature of the sample was probably not entirely uniform; the absolute accuracy of the measured dielectric properties at other than room temperatures is

questionable. For this reason we cannot accurately quote percentage errors at other than room temperatures. Summarized below (Table 4) are our results at 20° C compared to measured values by Von Hippel (1954) at comparable temperatures and frequencies.

Table 4

MATERIAL	CHIU (1974)		VON HIPPEL (1954)		
	ε_r'	tan δ	ε_r'	tan δ	
ERTALON	3.38	196×10^{-4}	—	—	—
	(f = 9.16 GH_z)				
TEFLON	2.04	6.6×10^{-4}	2.08	3.7×10^{-4}	t = 22° C f = 10 GH_z *pp.* 332
	(f = 8.45 GH_z)				
PLEXIGLAS	2.54	71×10^{-4}	2.59	67×10^{-4}	t = 27° C f = 10 GH_z *pp.* 334
	(f = 8.61 GH_z)				
POLYSTRENE	2.53	3.1×10^{-4}	2.54	4.3×10^{-4}	t = 25° C f = 10 GH_z *pp.* 335
	(f = 9.217 GH_z)				

Part II of this thesis employs the methods of Part I to materials of unknown permittivty. Table 4 already quotes the results for pure polystyrene at room temperatures, and those at higher temperatures are given in § 11, Fig. 15 and 16. Also given in § 11, Figs. 18 & 19 are the values of ε_r' and ε_r'' for polystyrene doped with 0.1 ~ 2% of the polar molecule,

8-Quinolinol. Without additional data at other frequencies, it is not, of course, possible to state any conclusions about relaxation mechanisms for this molecule in the polystyrene matrix, but it is hoped that the present work will stimulate interest in carrying out similar measurements at other microwave bands. In this connection, it may be mentioned (Sing-Ting-Pay, McLellan; private communication) that measurements of ε_r' and ε_r'' for 10%, 8-Quinolinol in polystyrene at low frequencies ($10 \sim 100\ KH_z$) and low temperatures ($T = 77^\circ\ K$) indicate that there may be at least two relaxation mechanisms present: (i) the rotation of the 8-Quinolinol molecule in the highly viscous polystyrene background. This *inter*molecular effect is expected to give loss peaks in the KH_z region. (ii) internal rotation of the 8-Quinolinol dipole arising from *intra*molecular forces gives rise to losses which are expected to peak in the r.f. or microwave region.

Taken at various temperatures between that of liquid nitrogen ($77^\circ\ K$) and the glass-transition temperatures ($350^\circ\ K$), it is the latter mechanism which additional microwave measurements would help to illuminate.

Appendices A to J. Tables of Data.

Appendix A. Preliminary Measurements and Results of Pure Polystyrene at room temperature and f=9.547 GHz.

d (cm)	θ (degree)	α (db)	ε_r'	tan δ ($\times 10^{-4}$)
1.00	77.7	0.523	2.44	346.1
1.27	109.1	0.465	2.65	234.8
2.54	213.5	1.470	2.60	373.8
3.00	243.0	1.420	2.53	309.3
3.81	309.0	1.570	2.53	269.1
4.00	317.1	1.470	2.48	241.7
4.27	335.5	0.420	2.47	64.9
4.61	379.7	1.640	2.56	231.3
4.81	393.7	2.490	2.55	337.2
5.08	407.2	1.990	2.51	256.8
5.88	478.2	1.295	2.54	143.7
6.08	488.7	1.677	2.51	180.6
6.35	506.5	1.887	2.50	195.1
6.81	555.6	0.820	2.54	78.5
7.61	610.5	0.250	2.51	21.5
7.81	632.4	0.170	2.53	14.2
8.08	653.0	1.320	2.52	106.8
8.88	719.3	0.336	2.53	24.7
9.08	736.5	1.220	2.53	87.7
9.35	755.3	2.040	2.52	142.6

Appendix B. Additional Measurements of Pure Polystyrene at room temperature, by using half-wavelength samples of d=2.194 cm, and f=9.55 GHz.

d (cm)	θ (degree)	α (db)	ε_r'	$\tan\delta$ ($\times 10^{-4}$)
1.097	88.6	0.005	2.52	3.0
2.194	177.7	0.011	2.53	3.2
3.291	266.4	0.016	2.53	3.4
4.388	354.0	0.018	2.52	2.7
5.485	442.1	0.026	2.52	3.1
6.582	530.5	0.029	2.52	2.9

Appendix C. Dielectric Properties of Pure Polystyrene at f=9.217 GHz. and d=3 x $\lambda/2$ = 3.45 cm.

T°C	θ (degree)	α (db)	ε_r'	tan δ (x 10^{-4})
20.0	276.2	0.020	2.535	3.9
23.0	276.6	0.020	2.535	3.9
30.0	275.8	0.021	2.533	3.9
32.5	275.8	0.021	2.532	4.0
35.0	275.7	0.023	2.532	4.1
37.0	275.9	0.023	2.532	4.2
38.0	275.8	0.023	2.531	5.7
43.0	275.1	0.024	2.530	5.8
46.5	275.6	0.025	2.530	5.8
54.5	275.0	0.026	2.526	5.8
56.0	275.0	0.026	2.526	5.8
58.0	275.0	0.025	2.526	5.8
59.5	274.7	0.025	2.523	6.0
62.3	274.9	0.025	2.525	5.8
64.0	274.9	0.027	2.525	5.9
66.5	275.1	0.028	2.526	5.8
70.5	275.0	0.029	2.526	5.8
73.0	274.6	0.030	2.523	5.8

Appendix D. Dielectric properties of polystyrene with 0.1% of 8-Quinolinol, at f=9.217 GHz and $d=3\lambda/2$ = 3.46 cm.

T°C	θ (degree)	α (db)	ε'_r	tan δ (x 10^{-4})
19.5	277.4	0.087	2.544	16.8
21.0	276.7	0.088	2.538	17.0
29.0	276.5	0.092	2.537	17.8
35.0	276.6	0.097	2.538	18.8
36.0	276.5	0.100	2.537	19.4
37.5	276.4	0.104	2.536	20.1
44.5	276.4	0.120	2.536	23.2
47.5	276.4	0.125	2.536	24.2
48.0	276.5	0.126	2.537	24.4
53.0	276.3	0.136	2.535	26.3
55.5	276.2	0.140	2.535	27.1
58.0	276.1	0.143	2.534	27.7
61.5	276.0	0.155	2.533	30.0
64.0	276.1	0.155	2.534	30.0
69.0	275.9	0.155	2.532	30.0
70.5	275.8	0.155	2.532	30.0
72.0	275.7	0.155	2.531	30.0
73.0	275.3	0.155	2.528	30.1
74.0	275.1	0.150	2.526	29.1

Appendix E. Dielectric properties of polystyrene with 0.4% of 8-Quinolinol, at f=9.217 GHz and $d=3\lambda/2 = 3.46$ cm.

T°C	θ (degree)	α (db)	ε'_r	tan δ (x 10^{-4})
20.5	276.4	0.040	2.536	7.8
31.0	276.0	0.052	2.533	10.1
38.0	276.0	0.058	2.533	11.2
40.0	275.9	0.058	2.532	11.2
43.5	275.9	0.057	2.532	11.0
46.5	275.8	0.057	2.532	11.1
49.0	275.8	0.061	2.532	11.8
50.0	275.8	0.061	2.532	11.8
53.0	275.8	0.061	2.532	11.8
54.5	275.8	0.064	2.532	12.4
57.0	275.7	0.064	2.531	12.4
58.5	275.6	0.065	2.530	12.6
61.0	275.7	0.065	2.531	12.6
62.0	275.5	0.067	2.529	13.0
68.0	275.4	0.075	2.529	14.5
69.0	275.2	0.081	2.527	15.7
71.5	275.1	0.085	2.526	16.5
74.0	274.9	0.087	2.525	16.9

Appendix F. Dielectric Properties of polystyrene with 0.8% of 8-Quinolinol, at f=9.217 GHz and d=3 x $\lambda/2$ = 3.46 cm.

T°C	θ (degree)	α (db)	ϵ_r'	tan δ (x 10^{-4})
23.0	277.6	0.120	2.545	23.2
39.5	277.4	0.141	2.544	27.3
41.0	277.3	0.145	2.543	28.1
43.0	277.2	0.159	2.542	28.8
44.0	277.2	0.150	2.542	29.0
45.0	277.2	0.150	2.542	29.0
47.0	277.1	0.152	2.541	29.4
49.5	277.0	0.155	2.541	30.0
50.5	277.1	0.155	2.541	30.0
52.5	277.2	0.159	2.542	30.8
55.0	277.0	0.163	2.541	31.5
60.5	276.9	0.170	2.540	32.9
61.5	276.0	0.172	2.540	33.3
64.5	276.8	0.172	2.541	33.3
68.5	276.9	0.177	2.539	34.3
69.5	276.9	0.180	2.540	34.9
71.0	276.6	0.182	2.540	35.2
73.0	276.	0.182	2.538	35.2

Appendix G. Dielectric properties of polystyrene with 1% of 8-Quinolinol, at f=9.217 GHz and d=3λ/2 = 3.46 cm.

T°C	θ (degree)	α (db)	ε'_r	tan δ (x 10^{-4})
20.5	278.5	0.140	2.552	27.1
24.5	278.0	0.140	2.548	27.1
36.0	278.0	0.150	2.548	29.0
39.0	278.1	0.155	2.549	30.0
40.5	277.9	0.160	2.547	30.9
43.0	277.9	0.160	2.547	30.9
46.0	277.8	0.160	2.547	30.9
49.5	277.7	0.175	2.546	33.8
51.0	277.7	0.180	2.546	34.8
53.0	277.6	0.180	2.545	34.8
62.0	277.7	0.200	2.546	38.7
66.0	277.7	0.205	2.546	39.6
68.0	277.9	0.213	2.547	41.2
72.0	278.9	0.218	2.547	42.1
73.0	278.0	0.220	2.548	42.5
73.5	278.0	0.222	2.548	42.9

Appendix H. Dielectric properties of polystyrene with 1.4% of 8-Quinolinol, at f=9.217 GHz and d=3λ/2 = 3.46 cm.

$T^{o}C$	(degree)	(db)	ε'_r	tan δ (x 10^{-})
20.0	280.4	0.170	2.566	32.8
29.0	280.9	0.177	2.570	34.1
30.0	280.8	0.182	2.569	35.1
33.0	280.5	0.186	2.568	35.9
34.5	280.4	0.190	2.566	36.6
36.0	280.3	0.190	2.565	36.6
39.0	280.2	0.193	2.565	37.2
42.5	280.3	0.198	2.565	38.2
47.0	280.0	0.202	2.563	39.0
50.0	280.1	0.205	2.564	39.5
52.5	280.1	0.210	2.564	40.5
57.0	280.2	0.222	2.565	42.8
60.0	280.1	0.230	2.564	44.4
65.0	280.0	0.235	2.563	45.3
70.5	278.6	0.246	2.553	47.5
75.0	278.6	0.254	2.553	49.1

Appendix I. Dielectric properties of polystyrene with 1.8% of 8-Quinolinol, at f=9.217 GHz and d=3 x $\lambda/2$ = 3.46 cm.

T°C	θ (degree)	α (db)	ε'_r	tan δ ($\times 10^{-4}$)
25.0	281.1	0.260	2.571	50.1
37.0	281.2	0.268	2.572	51.6
39.0	281.2	0.273	2.572	52.6
40.0	281.4	0.275	2.574	53.0
43.5	281.3	0.280	2.573	53.9
45.0	281.4	0.290	2.574	55.9
49.0	281.4	0.292	2.574	56.2
50.0	281.5	0.300	2.574	57.8
53.0	281.4	0.300	2.574	57.8
55.0	281.3	0.320	2.573	61.6
57.0	281.2	0.322	2.572	62.0
58.5	281.2	0.330	2.572	63.6
60.0	281.2	0.330	2.572	63.6
63.0	281.0	0.340	2.571	66.5
65.5	281.0	0.345	2.570	66.5
67.0	280.9	0.350	2.570	67.4
68.0	280.7	0.380	2.568	73.2
69.0	279.4	0.385	2.558	74.3
72.0	278.8	0.395	2.554	76.3

Appendix J. Dielectric Properties of polystyrene with 2% of 8-Quinolinol, at f=9.217 GHz and d=3 x $\lambda/2$ = 3.46 cm.

T°C	θ (degree)	α (db)	ε_r'	tan δ (x 10^{-4})
20.0	282.9	0.270	2.580	51.9
29.0	282.2	0.238	2.580	55.5
30.0	282.2	0.288	2.579	55.4
31.5	282.1	0.290	2.579	55.8
34.0	282.1	0.330	2.579	57.7
36.5	282.1	0.330	2.579	57.7
39.5	282.1	0.307	2.579	59.1
42.2	282.1	0.313	2.578	60.2
44.4	282.2	0.318	2.578	61.2
46.6	282.2	0.325	2.578	62.6
49.5	282.2	0.375	2.578	72.2
53.0	281.9	0.344	2.577	66.2
55.5	281.9	0.355	2.577	68.3
58.5	281.8	0.363	2.576	69.9
61.5	281.7	0.380	2.576	73.2
63.5	281.7	0.392	2.576	75.5
65.0	281.8	0.405	2.576	78.0
68.0	281.8	0.420	2.576	80.9
73.0	281.9	0.435	2.577	83.7
74.0	281.9	0.440	2.577	84.7

REFERENCES

Barnes, Thomas G., "Foundations of Electricty and Magnetism", Schellanger Research Laboratories, Texas Western College of the Universtiy of Texas, P. 285, 1965.

Bronwell, Arthur B., Robert E. Beam, "Theory and Application of Microwave", McGraw-Hill, P. 261, 1947.

Brydon, J. A., "Plastic Materials", 2nd edition, Iliffe Books Ltd., London, P. 28, 1969.

Debye, P., "Polar Molecules", Dover Publications, P. 94, 1929.

Fröhlich, H., "Theory of Dielectrics", 2nd edition, Oxford University Press, P. 105 & 113, 1958.

Frood, D. G., & Fuller, P. W. (1964), Characteristics of X - band Microwave Apparatus for Wake Studies in a Hypervelocity Range. R.A.R.D.E., Memorandum 42/64.

Harvey, A. F., "Microwave Engineering", Academic Press London and New York, P. 239, 1963.

McCellan, A. L. "Tables of Experimental Dipole Moments", W. H. Freeman and Company, San Fransico and London, P. 320, 1963.

Montgomery, Carol G., "Technique of Microwave Measurements", Vol. 2, New York, Dover Publication, P. 561, 1966.

Moore, Robert D., "Lock-in Amplifier for Signals Buried in Noise", Princeton Applied Research Corp., Princeton, N.J. 1962.

Symth, Charles Phelps, "Dielectric Behavior and Structure", McGraw-Hill, P. 63 & 183, 1955.

Von Hippel, Arthur Robert, "Dielectric Materials and Applications", New York, Wiley, P. 220, 332-336, 1954.

Wheeler, Gershon J., "Introduction to Microwaves", Prentice-Hall Inc., Englewood Cliffs, N. J., P. 13, 1963.

Wind, Moe, Harold Rapaport, "Hand Book of Microwave Measurements", Vol. 1, P. 499, 1955.